THE JOURNAL OF BIOLOGICAL CHEMISTRY VOL. 290, NO. 50, pp. 29854–29868, December 11, 2015

The Nuclear Factor (Erythroid-derived 2)-like 2 and Proteasome Maturation Protein Axis Mediate Bortezomib Resistance in Multiple Myeloma*

Received for publication, May 13, 2015, and in revised form, September 28, 2015 Published, JBC Papers in Press, October 19, 2015, DOI 10.1074/jbc.M115.664953

Bingzong Li[‡§1], Jinxiang Fu[‡], Ping Chen[‡], Xueping Ge[‡], Yali Li[‡], Isere Kuiatse[§], Hua Wang[§], Huihan Wang[§], Xingding Zhang[§], and Robert Z. Orlowski[§¶2]

From the [‡]Department of Hematology, Second Affiliated Hospital of Soochow University, Suzhou 215006, Jiangsu, China and the Departments of [§]Lymphoma and Myeloma and [¶]Experimental Therapeutics, The University of Texas MD Anderson Cancer Center, Houston, Texas 77030

Background: Acquired proteasome inhibitor resistance emerges in myeloma patients through incompletely understood mechanisms.
Results: Activation of nuclear factor (erythroid-derived 2)-like 2 (*NRF2*) and proteassemblin (*POMP*) was linked to bortezomib resistance, while their inhibition reversed resistance.
Conclusion: The *NRF2/POMP* axis contributes to bortezomib resistance.
Significance: *NRF2/POMP* axis inhibition can be translated to the clinic to reverse bortezomib resistance and induce chemosensitization.

Resistance to the proteasome inhibitor bortezomib is an emerging clinical problem whose mechanisms have not been fully elucidated. We considered the possibility that this could be associated with enhanced proteasome activity in part through the action of the proteasome maturation protein (POMP). Bortezomib-resistant myeloma models were used to examine the correlation between POMP expression and bortezomib sensitivity. POMP expression was then modulated using genetic and pharmacologic approaches to determine the effects on proteasome inhibitor sensitivity in cell lines and *in vivo* models. Resistant cell lines were found to overexpress POMP, and while its suppression in cell lines enhanced bortezomib sensitivity, POMP overexpression in drug-naive cells conferred resistance. Overexpression of POMP was associated with increased levels of nuclear factor (erythroid-derived 2)-like (NRF2), and NRF2 was found to bind to and activate the *POMP* promoter. Knockdown of *NRF2* in bortezomib-resistant cells reduced POMP levels and proteasome activity, whereas its overexpression in drug-naive cells increased POMP and proteasome activity. The NRF2 inhibitor all-*trans*-retinoic acid reduced cellular NRF2 levels and increased the anti-proliferative and pro-apoptotic activities of bortezomib in resistant cells, while decreasing proteasome capacity. Finally, the combination of all-*trans*-retinoic acid with bortezomib showed enhanced activity against primary patient samples and in a murine model of bortezomib-resistant myeloma. Taken together, these studies validate a role for the *NRF2/POMP* axis in bortezomib resistance and identify *NRF2* and *POMP* as potentially attractive targets for chemosensitization to this proteasome inhibitor.

Inhibition of the function of the ubiquitin-proteasome pathway with the proteasome inhibitor bortezomib is an accepted standard of care for the treatment of relapsed and/or refractory multiple myeloma both alone (1, 2) and as part of rationally designed combination regimens (3). In addition, bortezomib-based therapies have been incorporated into the front-line setting for patients with newly diagnosed myeloma (4–7) and are being considered in other settings as well, including as part of maintenance therapy (8). Indeed, together with other advances, such as the development of immunomodulatory agents, bortezomib has contributed to a doubling in the overall survival of myeloma patients over the last decade (9–12). Myeloma cells may be especially sensitive to proteasome inhibitors because protein turnover capacity is reduced during plasma cell differentiation (13). This increases proteasome load relative to capacity, thereby triggering cellular stress and enhancing reliance on the unfolded protein response for survival, which is easily overwhelmed by proteasome inhibitors through their rapid induction of ubiquitin-protein conjugates. Indeed, the ratio of proteasome load to capacity may determine apoptotic sensitivity to bortezomib, with plasma cells having a high load

* This work was supported in part by National Institutes of Health Grant P50 CA142509 (to MD Anderson Cancer Center SPORE in Multiple Myeloma), National Institutes of Health Cancer Center Support Grant CA16672 (to MD Anderson Characterized Cell Line Core Facility). R. Z. O. has served on advisory boards for Millennium: The Takeda Oncology Co., which developed and markets bortezomib, and for Onyx Pharmaceuticals, which developed and markets carfilzomib, and has received research funding from both entities; however, these funds did not support the current line of investigation. The content is solely the responsibility of the authors and does not necessarily represent the official views of the National Institutes of Health.
[1] Supported by National Natural Science Foundation of China Grants 81172256 and 81272631, Applied Basic Research Programs of Suzhou City Grant SYS201546, and China Postdoctoral Science Foundation-funded Project 2014M550307.
[2] Supported by the Florence Maude Thomas Cancer Research Professorship, National Institutes of Health Grants R01 CA184464 and CA194264, the Brock Family Myeloma Research Fund, the Yates Ortiz Myeloma Fund, the Jay Solomon Myeloma Research Fund, and the Diane and John Grace Family Foundation. To whom correspondence should be addressed: Dept. of Lymphoma and Myeloma, The University of Texas MD Anderson Cancer Center, 1515 Holcombe Blvd., Unit 429, Houston, TX 77030-4009. Tel.: 713-794-3234; Fax: 713-563-5067; E-mail: rorlowsk@mdanderson.org.

TABLE 1

Characteristics of myeloma patients whose primary plasma cells were studied

The following abbreviations are used: M, male; F, female; ISS, International Staging System; DS, Durie-Salmon Staging System; VAD, vincristine, doxorubicin, and dexamethasone; MP, melphalan plus prednisone; PAD, bortezomib, doxorubicin, plus dexamethasone; VMP, bortezomib, melphalan, and prednisone; VDT, bortezomib, dexamethasone, and thalidomide; DVD, pegylated liposomal doxorubicin, vincristine, and dexamethasone; MPR, melphalan, prednisone, and lenalidomide; M2, carmustine, vincristine, cyclophosphamide, melphalan, and prednisone. [a], 2 months before sample collection; [b], 4 months before sample collection; [c], 6 months before sample collection; [d], 6 months before sample collection; [e], 1 year before sample collection; [f], 4 years before sample collection.

Patient no.	Sex	Age	Clinical stage (ISS)	Clinical stage (DS)	Previous treatment	Para protein	Percentage of plasma cells	Bone lesions
		year					*%*	
MM1	F	59	I	IIIA	No	IgG-κ	19.0	Yes
MM2	M	74	II	IIIA	No	IgG-κ	58.0	Yes
MM3	F	58	II	IIIA	No	IgG-κ	16.0	Yes
MM4	F	66	II	IIIA	VAD × 6; MP × 2[a]	Non-secretary	90.0	Yes
MM5	M	69	III	IIIB	PAD × 1; VMP × 3; VDT × 3[b]	λ-Light Chain	80.0	Yes
MM6	M	81	III	IIIB	PAD × 1[c]	IgG-λ	5.0	No
MM7	M	67	III	IIIA	DVD × 5; MPR × 1; VDT × 2; M2 × 1[d]	IgG-λ	37.0	Yes
MM8	M	65	III	IIIA	VAD × 6[e]	λ-Light Chain	60.0	Yes
MM9	M	84	III	IIIB	VDT × 2[f]	IgG-λ	55.0	Yes
MM10	M	73	III	IIIA	No	IgG-κ	93.0	Yes
MM11	F	64	II	IIA	No	IgG-λ	19.0	No
MM12	M	64	I	IIIA	No	IgG-κ	16.0	Yes

and/or low capacity showing sensitivity (14). However, even in patients whose disease initially responds very well to bortezomib, resistance eventually develops in the majority, thereby limiting the reuse of regimens that were previously successful (15–17).

Initial studies in leukemia cell lines described a role for overexpression of the β5 proteasome subunit targeted by bortezomib and showed that shRNA-mediated knockdown of β5 to some extent restored bortezomib sensitivity (18–20). Also, mutations in the β5 subunit's bortezomib binding pocket were implicated in acquired bortezomib resistance (18–20). However, free β5 subunits are catalytically inactive and contain a pro-sequence that would preclude bortezomib binding (21, 22), and β5 mutations were later found to be absent from patient-derived samples (23, 24). A more recent study demonstrated that proteasome inhibitor resistance occurred through emergence of plasmablasts with reduced immunoglobulin production (25). These precursor cells have a decreased proteasome load and better balance between load and capacity, thereby reducing cellular stress and apoptotic sensitivity. If this were the only mechanism of acquired resistance, however, all refractory patients would have oligo-secretory or non-secretory myeloma, which is not the case (15–17). We therefore approached this area with the hypothesis that increased proteasome capacity could cause resistance by also modulating the load/capacity ratio in a manner that would reduce cell stress (26). Moreover, we considered the possibility that this could occur by enhancing the efficiency of assembly of the 20S proteasome core particle. This occurs through the coordinated action of proteasome assembly chaperones 1–4 and of proteasome maturation protein (POMP,[3] proteassemblin) (21, 22), and because the latter is responsible for assembly of the catalytically active β subunit rings, we focused on this chaperone.

In this study, using previously established and validated myeloma models of bortezomib resistance (27), we report findings demonstrating that POMP overexpression is indeed associated with resistance. Its expression was sufficient by itself to confer resistance, and *POMP* activation was associated with induction of an upstream transcription factor, nuclear factor, erythroid 2-like 2 (*NRF2*), and with enhanced proteasome activity. Finally, suppression of either *NRF2* or *POMP* using either short hairpin (sh) RNAs or a pharmacologic agent restored sensitivity in cell lines, primary plasma cells, and an *in vivo* myeloma model.

Experimental Procedures

Cell Lines and Primary Samples—Drug-naive and bortezomib-resistant myeloma cell lines were developed and maintained as described previously (27). Cell line authentication was performed by our cell line characterization core using short tandem repeat profiling. Bortezomib was removed from the culture for at least 7 days prior to all experiments, unless indicated otherwise, to negate the possibility that proteasome inhibitor-induced oxidative stress was impacting *NRF2* and *POMP* expression. Primary plasma cells were purified from bone marrow aspirates collected from patients under an approved protocol from the Institutional Review Board at the Second Affiliated Hospital of Soochow University after informed consent was obtained in compliance with the Declaration of Helsinki. The clinical history, including prior treatments, of the patients whose samples were used is shown in Table 1.

Viability Assays—Proliferation and viability assays with bortezomib (Selleck Chemical, Houston, TX) and all-*trans*-retinoic acid (ATRA) (Sigma) were performed as described previously (28). Briefly, cell lines or primary samples were treated with the indicated compound for a minimum of 24 h, unless otherwise indicated, followed by the addition of the tetrazolium reagent WST-1. Colorimetric detection of metabolic activity was then obtained on a Victor3V plate reader (PerkinElmer Life Sciences). Data were normalized to vehicle controls, which were arbitrarily set at 100% viability, and all data points are represented as the mean with the standard deviation (S.D.).

Immunoblotting—Cells were harvested and lysed in 1× Lysis Buffer (Cell Signaling Technology, Danvers, MA), followed by resolution on gradient gels (Thermo Fisher Scientific, Carlsbad, CA), transferred to nitrocellulose (Bio-Rad), and probed with

[3] The abbreviations used are: POMP, proteasome maturation protein; ATRA, all-*trans*-retinoic acid; OE, overexpression; qPCR, quantitative PCR; NT, non-targeting.

the indicated antibodies. Primary anti-POMP, anti-NRF2, anti-Kelch-like ECH-associated protein 1 (KEAP1) and anti-cleaved caspase 3 antibodies were from Cell Signaling Technology (Beverly, MA); the 20S proteasome β5 subunit (PSMB5) antibody was from Santa Cruz Biotechnology, and anti-β-actin was from Sigma. Densitometric quantitation was obtained using ImageJ software (National Institutes of Health, rsbweb.nih.gov) and normalized to β-actin and either vehicle-treated or wild-type controls, which were arbitrarily set to 1.

Real Time RT-PCR—Real time PCR was carried out as described previously, with some modifications (28). Briefly, total RNA was isolated from cultured cells or tumor tissues using TRIzol (Thermo Fisher Scientific), and cDNA was synthesized using a High Capacity cDNA reverse transcription kit (Applied Biosystems, Foster City, CA). Quantitative (q) real time PCR was performed using the TaqMan Gene Expression Master Mix and the *POMP* (FAM™), *NRF2* (FAM™), proteasome *β5* subunit, and glyceraldehyde 3-phosphate dehydrogenase (GAPDH, VIC®) TaqMan gene expression assays as multiplexed, triplicate samples on a StepOnePlus PCR system (Applied Biosystems). Relative quantification was done using the comparative C_T method after normalization to the internal GAPDH control, where all samples were then normalized to wild-type or vehicle controls.

POMP and NRF2 Silencing—Six lentivirus-based shRNAs targeted to *POMP*, eight lentivirus-based shRNAs targeted to *NRF2*, or a nonspecific scrambled control (Sigma) were transfected with the packaging vectors psPAX2 and pMD2.G into 293T cells by calcium chloride to produce the lentiviruses. Two days later, the supernatants were collected, filtered, concentrated, and used for experiments or frozen at −80 °C. KAS-6/1 bortezomib-resistant (V10R) and OPM-2 V10R cells were transduced by using lentiviruses with Polybrene (8 μg/ml, Sigma) and infected cells were selected with 2 μg/ml puromycin. The expression of POMP or NRF2 was determined by Western blot analysis and real time PCR. Two of the lentivirus-based shRNAs targeted to *POMP*, constructs 3 and 5, and two for *NRF2*, constructs 6 and 8, were validated for further studies. *POMP* shRNA lentiviral vectors contained two target-specific constructs, CCGGGGGTCTATTTGCTCCGCTAAACTCGAGTTTAGCGGAGCAAATAGACCCTTTTTG and CCGGCTATTGGATTTGAGGATATTCCTCGAGGAATATCCTCAAATCCAATAGTTTTTG. *NRF2* shRNA lentiviral vectors also contained two target-specific constructs, CCGGGCACCTTATATCTCGAAGTTTCTCGAGAAACTTCGAGATATAAGGTGCTTTTT and CCGGCCGGCATTTCACTAAACACAACTCGAGTTGTGTTTAGTGAAATGCCGGTTTTT. Sequences from *POMP* construct 3 were then also used in some transient transfection assays to knock down *POMP* without subsequent antibiotic selection. Non-targeting shRNAs (KO-NT) or shRNAs targeting *POMP* (KO-3) were introduced by electroporation using the Neon® transfection system (Thermo Fisher Scientific).

POMP and NRF2 Expression—pCMV6-XL5 vectors containing *POMP* or *NRF2* cDNAs were purchased from OriGene (Rockville, MD). *POMP* or *NRF2* was subcloned into the lentiviral vector transfer plasmid pCDH-CMV-MCS-EF1-coGFP to generate pCDH-CMV-POMP-EF1-coGFP or pCDH-CMV-NRF2-EF1-coGFP. The recombinant pCDH-CMV-POMP-EF1-coGFP vector, pCDH-CMV-NRF2-EF1-coGFP vector, or the control vector pCDH-CMV-MCS-EF1-coGFP was transfected with the packaging vectors psPAX2 and pMD2.G into 293T cells by calcium chloride to produce lentiviruses. KAS-6/1 and OPM-2 cells were infected with control or either *POMP*- or *NRF2*-expressing lentiviruses, and expression was verified by qPCR and Western blotting.

Proteasome Activity Assays—Chymotrypsin-like proteasome activity was assayed in a total volume of 200 μl using 96-well plates performed according to the manufacturer's instructions (Promega, Madison, WI). Briefly, Proteasome-Glo™ cell-based reagent was prepared by reconstituting the luciferin detection reagent, Proteasome-Glo™ cell-based buffer, and the Suc-LLVY-Glo™ substrate was then added to an equal volume of samples containing 15,000 cells and incubated for a minimum of 5–10 min before luminescence measurements.

Chromatin Immunoprecipitation (ChIP)—Cells were first cross-linked with 2% paraformaldehyde for 10 min at 37 °C and sonicated. DNA-protein complexes were isolated with a ChIP assay kit (EMD Millipore, Billerica, MA) according to the manufacturer's instructions with antibodies against NRF2 (Abcam, Cambridge, MA). The precipitated DNA was purified and quantified by real time PCR. Primers used were as follows: 5′-CCTCCAACCTCATCTCAT-3′ (forward) and 5′-CTGAATAGCTGGGACTACA-3′ (reverse). The results were normalized relative to the input control.

Luciferase Assay—Luciferase reporter assays were performed using the LightSwitch Dual Assay System (SwitchGear Genomics, Carlsbad, CA) according to the manufacturer's instructions. KAS-6/1 and KAS-6/1 V10R cells were transiently transfected in triplicate with either empty-luciferase or *POMP*-luciferase, along with a *Cypridina* TK control construct and empty pCMV6-XL5 vector or pCMV6-XL5-NRF2 by electroporation using the Neon® transfection system (Thermo Fisher Scientific). The *Renilla* luciferase/*Cypridina* luciferase ratio was calculated to normalize for transfection efficiency.

Electrophoretic Mobility Shift Assay—DNA-protein binding assays were carried out with nuclear extract from KAS-6/1 V10R cells with 3′-biotinylated synthetic complementary oligonucleotides (Sigma). The sequence of the oligonucleotide used was 5′-CTCCAGCCTAGGTGACACAGCAAGA-3′, and the labeled oligonucleotides were annealed by mixing equal molar amounts of the two single-stranded oligonucleotides, heating to 95 °C for 5 min, followed by ramp cooling to 25 °C over a period of 45 min. Nuclear extracts were prepared using the nuclear/cytosol fractionation kit (BioVision, Carlsbad, CA) following the manufacturer's instructions. Binding reactions were carried out for 20 min at room temperature in the presence of 50 ng/μl poly(dI-dC), 0.05% Nonidet P-40, 5 mM $MgCl_2$, 10 mM EDTA, and 2.5% glycerol in 1× binding buffer using 20 fmol of biotin end-labeled target DNA and 4 μg of nuclear extract. Additionally, 4 pmol of unlabeled probe was added to some binding reactions as a specific competitor DNA. Assays were loaded onto native 4% polyacrylamide gels pre-electrophoresed for 60 min in 0.5× Tris borate/EDTA and electrophoresed at 100 V before being transferred onto a positively charged nylon membrane in 0.5× Tris borate/EDTA at 100 V for 30 min.

Transferred DNAs were cross-linked to the membrane at 120 mJ/cm^2 and detected using horseradish peroxidase-conjugated streptavidin according to the manufacturer's instructions using the LightShift chemiluminescent EMSA kit (Thermo Fisher Scientific).

Xenograft Modeling—Bortezomib-resistant KAS-6/1 cells (7×10^6 cells/mouse) were subcutaneously xenografted into 6-week-old non-obese diabetic/severe combined immunodeficiency (NOD/SCID) mice (NOD.Cg-Prkdc(scid) Il2rg(tm1Wjl)/SzJ; The Jackson Laboratory, Bar Harbor, ME) with Matrigel (BD Biosciences, San Jose, CA) under a protocol approved by the institutional Animal Care and Use Facility. The mice were randomized into four groups with five subjects in each cohort, and treatments were administered by intraperitoneal injection using peanut oil as a carrier three times weekly, starting on day 7 post-implantation. Tumors were monitored by caliper measurement, and tumor volume was determined using the equation volume $= 0.4l \times w^2$. The CONTRAST statement in PROC MIXED procedure in SAS (SAS Institute, Inc., Cary, NC) was used to compare the tumor growth rates between each pair of groups. The tumor volume was log-transformed to satisfy the normality assumption of the models. Tumors were removed for qPCR or Western blot assays at the indicated time point. Pairwise differences between the combination group (bortezomib + ATRA) *versus* ATRA alone, combination *versus* bortezomib, combination *versus* control, bortezomib *versus* control, and ATRA *versus* control were examined using the ESTIMATE statement in PROC MIXED for each time point. Statistically significant determinations were made by calculation of the probability of χ^2.

Results

Bortezomib-resistant Cells Overexpress POMP—Previous studies from our group determined that bortezomib-resistant myeloma cells exposed to proteasome inhibitors showed a more rapid recovery of the chymotrypsin-like proteasome activity (27). We considered the possibility that this could be due to more rapid assembly of new proteasomes and increased proteasome capacity, and analysis of gene expression profiling data comparing bortezomib-resistant cells with their sensitive counterparts revealed up-regulation of *POMP* (data not shown). To further validate these findings, we performed qPCR comparing bortezomib-resistant (V10R) RPMI 8226, OPM-2, ANBL-6, and KAS-6/1 cells with their wild-type (WT), vehicle-treated, and drug-naive counterparts passaged in parallel. Bortezomib-resistant cells consistently showed enhanced *POMP* mRNA levels in each of the cell line models studied (Fig. 1*A*), with, for example, up to a 10-fold increase in RPMI 8226 V10R cells compared with their WT controls. These enhanced messenger levels led to an increased accumulation of POMP protein as judged by Western blotting (Fig. 1*B*), with up to a 6-fold increase, for example, in the RPMI 8226 cells. Finally, to determine whether POMP levels were increased in primary samples, Western blotting was performed on CD138$^+$ plasma cells from four bortezomib-naive patients and three bortezomib-resistant patients. The latter showed a consistently higher POMP expression level (Fig. 1*C*), supporting the hypothesis that higher POMP levels may be associated with bortezomib resistance.

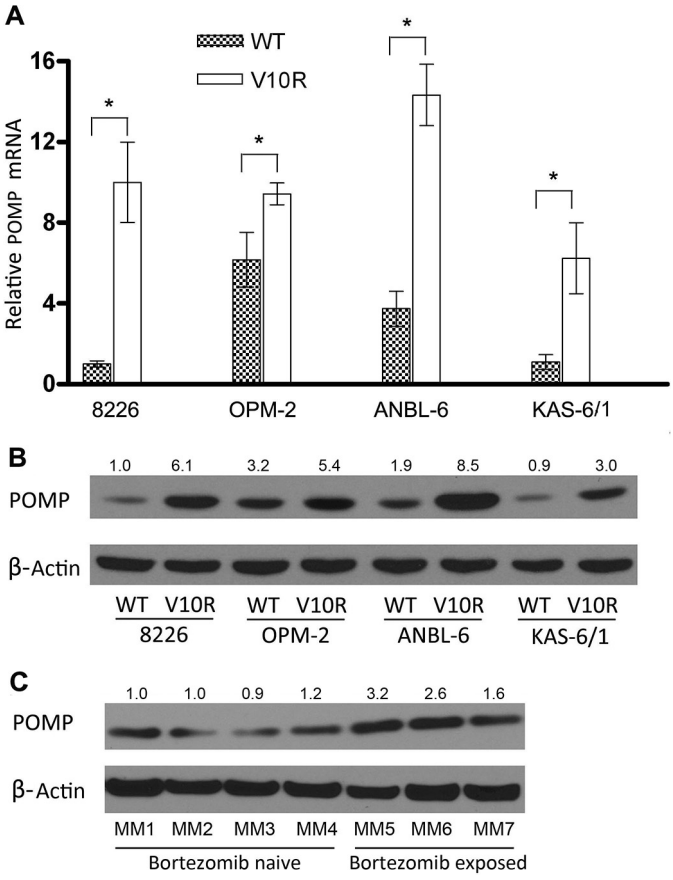

FIGURE 1. **Bortezomib resistance and *POMP* levels in myeloma cell lines.** *A,* bortezomib-sensitive (WT) and bortezomib-resistant (V10R) myeloma cell lines, including RPMI 8226 (8226), OPM-2, ANBL-6, and KAS-6/1 cells, were subjected to qPCR to detect *POMP* mRNA content, which was analyzed using the comparative C_T method and normalized to GAPDH as an internal control. *POMP* expression in drug-naive 8226 cells was arbitrarily set at 1.0, and data are provided from three independently performed experiments ± standard deviation. The Student's paired *t* test was used to determine statistical significance (*, $p < 0.05$ *versus* WT). *B,* POMP protein levels were evaluated in these same cell lines by immunoblotting and compared with β-actin as a loading control. Densitometry was performed to quantify POMP levels, which were normalized to RPMI 8226 WT cells arbitrarily set to 1.0. A representative autoradiograph is shown from one of two independently performed experiments. *C,* POMP and β-actin levels are shown by Western blotting in primary plasma cells from four patients who were bortezomib-naive and three patients who were previously bortezomib-exposed and clinically bortezomib-refractory. Densitometry was performed to quantify POMP levels, which were normalized to MM1 cells arbitrarily set to 1.0.

POMP Modulates Bortezomib Sensitivity—Because a number of mechanisms may be simultaneously activated to confer bortezomib resistance in myeloma cell lines, we sought to confirm that changes in *POMP* were alone sufficient to modulate sensitivity. We therefore generated KAS-6/1 V10R cells infected with lentiviral vectors expressing either a control, non-targeting (NT) shRNA, or one of two different shRNAs that successfully suppressed *POMP* (KO-3 and KO-5) (Fig. 2*A*). When these cells were then treated with either vehicle or bortezomib, compared with the parental KAS-6/1 V10R and NT controls, the KO-3 and -5 cells with lower levels of POMP were consistently more sensitive to proteasome inhibition (Fig. 2*B*). Moreover, the resistance to bortezomib in V10R cells almost fully reversed to the levels of KAS-6/1 wild-type (WT) cells (Fig. 2*B*), which was associated with inhibited proteasome chymot-

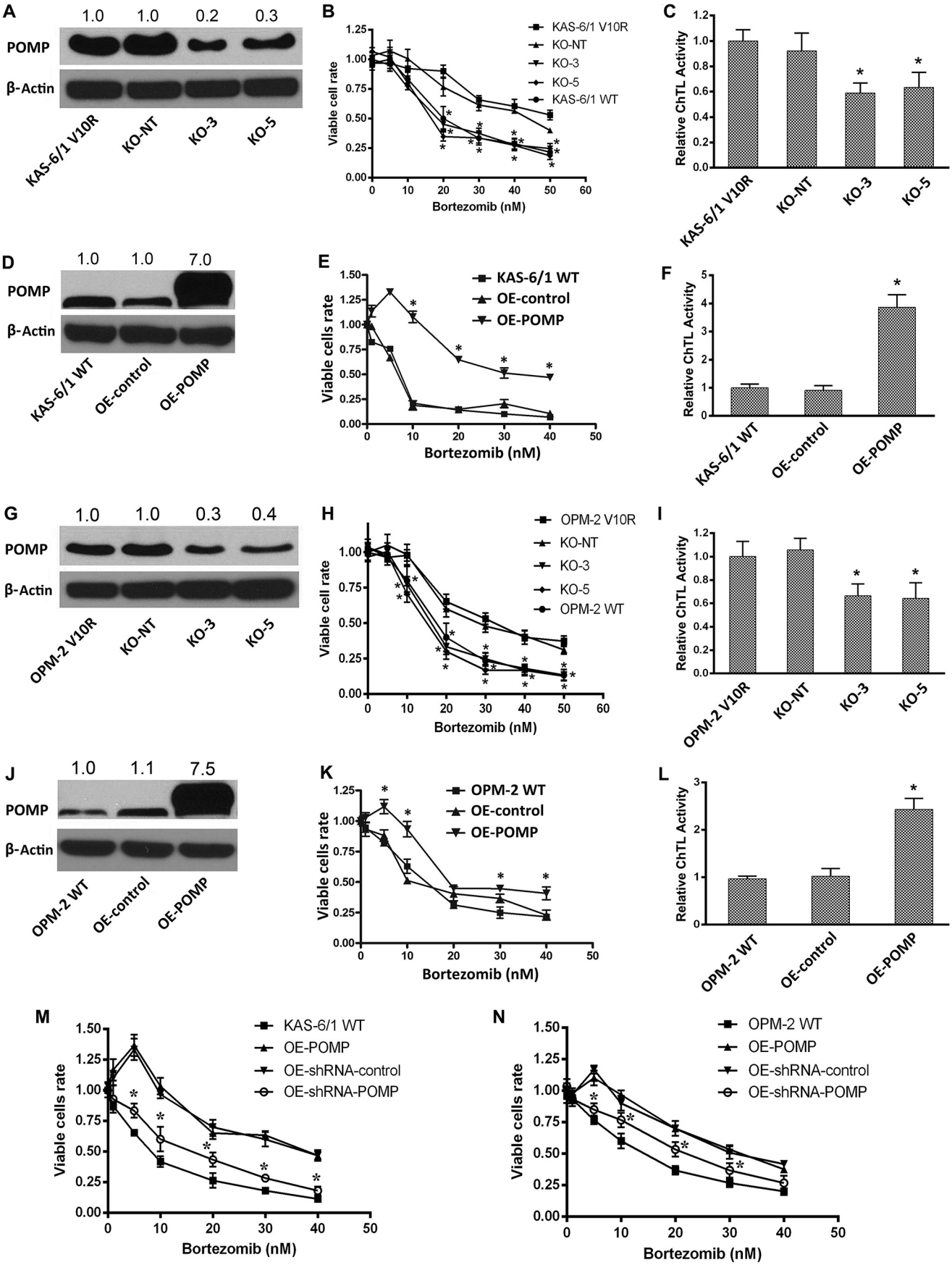
A
1.0 1.0 0.2 0.3
POMP
β-Actin
KAS-6/1 V10R
KO-NT
KO-3
KO-5
B
KAS-6/1 V10R
KO-NT
KO-3
KO-5
KAS-6/1 WT
Viable cell rate
Bortezomib (nM)
C
Relative ChTL Activity
KAS-6/1 V10R
KO-NT
KO-3
KO-5
D
1.0 1.0 7.0
POMP
β-Actin
KAS-6/1 WT
OE-control
OE-POMP
E
KAS-6/1 WT
OE-control
OE-POMP
Viable cells rate
Bortezomib (nM)
F
Relative ChTL Activity
KAS-6/1 WT
OE-control
OE-POMP
G
1.0 1.0 0.3 0.4
POMP
β-Actin
OPM-2 V10R
KO-NT
KO-3
KO-5
H
OPM-2 V10R
KO-NT
KO-3
KO-5
OPM-2 WT
Viable cell rate
Bortezomib (nM)
I
Relative ChTL Activity
OPM-2 V10R
KO-NT
KO-3
KO-5
J
1.0 1.1 7.5
POMP
β-Actin
OPM-2 WT
OE-control
OE-POMP
K
OPM-2 WT
OE-control
OE-POMP
Viable cells rate
Bortezomib (nM)
L
Relative ChTL Activity
OPM-2 WT
OE-control
OE-POMP
M
KAS-6/1 WT
OE-POMP
OE-shRNA-control
OE-shRNA-POMP
Viable cells rate
Bortezomib (nM)
N
OPM-2 WT
OE-POMP
OE-shRNA-control
OE-shRNA-POMP
Viable cells rate
Bortezomib (nM)

rypsin-like activity (Fig. 2*C*). To confirm these findings further, we compared OPM-2 V10R and NT cells that had high levels of POMP expression with OPM-2 KO-3 and -5 cells (Fig. 2*G*). As had been the case in the KAS-6/1 models, OPM-2 cells with lower levels of POMP were more sensitive to rechallenge with bortezomib, which produced a greater decline in viability (Fig. 2*H*) and chymotrypsin-like activity (Fig. 2*I*).

It also was of interest to determine whether overexpression of POMP was by itself able to confer a bortezomib-resistant phenotype. To that end, we used drug-naive KAS-6/1 WT cells and constructed clones that bore either the empty overexpression vector (OE-control) or *POMP* (OE-POMP) (Fig. 2*D*). Contrary to what was seen with POMP suppression, when POMP was overexpressed, bortezomib resistance (Fig. 2*E*) and enhanced chymotrypsin-like activity (Fig. 2*F*) were seen in KAS-6/1 cells. Notably, overexpression of POMP in OPM-2 cells (Fig. 2*J*) similarly reduced sensitivity to bortezomib (Fig. 2*K*) and enhanced chymotrypsin-like activity (Fig. 2*L*), indicating that *POMP* is indeed a modulator of proteasome inhibitor sensitivity.

To further examine whether POMP levels were associated with bortezomib resistance, *POMP*-overexpressing (POMP-OE) KAS-6/1 cells (Fig. 2*M*) and OPM-2 cells (Fig. 2*N*) were transiently transfected with non-targeting shRNAs (KO-NT) or with shRNAs targeting *POMP* (KO-3). Transfection with the *POMP* shRNAs consistently made the *POMP*-overexpressing cells more sensitive to proteasome inhibition than the non-targeting controls, although they did not return sensitivity to the level of WT cells because of incomplete *POMP* suppression (data not shown).

NRF2 Regulates POMP Expression—No direct inhibitors of *POMP* function have yet been described, and with the hope of finding an approach that could suppress *POMP* expression to sensitize bortezomib-resistant cells, we studied the POMP promoter and found a consensus binding site for NRF-2 within the −2833 to −2842 region. Also, a ChIP sequencing study in lymphoblastoid cells had suggested that the *POMP* promoter could be a target for NRF2 binding (29). To determine whether NRF2 indeed influenced *POMP* expression in myeloma cells, we first studied the bortezomib-resistant V10R cells by qPCR and found that, as had been the case for *POMP* (Fig. 1), they expressed higher levels of *NRF2* mRNA than their wild-type counterparts (Fig. 3*A*). In KAS-6/1 cells, for example, *NRF2* levels were increased almost 4-fold in the resistant *versus* the sensitive cells. Moreover, this resulted in higher levels of NRF2 protein expression, as determined by Western blotting comparing the V10R and WT cells (Fig. 3*B*). For example, again in the KAS-6/1 models, NRF2 levels were increased by 4-fold in the bortezomib-resistant cells. To determine whether NRF2 levels were increased in primary samples, Western blotting was performed on $CD138^+$ plasma cells from the same four bortezomib-naive patients and three bortezomib-resistant patients used earlier. The latter showed a relatively higher NRF2 expression level (Fig. 3*C*), supporting the hypothesis that higher NRF2 levels may be associated with higher POMP levels and bortezomib resistance.

NRF2, along with *KEAP1*, are parts of a signaling pathway that is important in cell defense and survival, including in response to anti-oxidant stress (30). Because *POMP* has also been linked to anti-oxidant defenses (31), this was another rea-

FIGURE 2. **Influence of *POMP* on bortezomib sensitivity.** *A,* KAS-6/1 bortezomib-resistant cells (*KAS-6/1 V10R*) were infected with lentiviral vectors expressing a scrambled sequence, non-targeting shRNA (*KO-NT*), or one of two different shRNAs targeting *POMP* (*KO-3* and *KO-5*). The success of *POMP* knockdown was verified with Western blotting and compared with β-actin as a loading control. Densitometry was performed to quantify POMP levels, which were normalized to KAS-6/1 V10R cells arbitrarily set to 1.0. A representative autoradiograph from one of two independent experiments is shown. *B,* cells described in *A* and KAS-6/1 drug-naive cells (*KAS-6/1 WT*) were then exposed to bortezomib for 24 h at the indicated concentrations, and viability was determined with the tetrazolium reagent WST-1. Data presented are from three independently performed experiments and are presented as the mean ± S.D. (*, $p < 0.05$ *versus* KAS-6/1 V10R or KO-NT). *C,* proteasome activity of the cells described in *A* was examined as described under "Experimental Procedures." Data are from three independent experiments and are presented as the mean ± SD. (*, $p < 0.05$ *versus* KAS-6/1 V10R or KAS-6/1 V10R KO-NT). *D,* KAS-6/1 drug-naive cells (*KAS-6/1 WT*) were infected with lentiviral vectors without a cDNA insert (*OE-control*) or the cDNA for *POMP* (*OE-POMP*). The success of POMP overexpression was verified with Western blotting and compared with β-actin as a loading control. Densitometry was performed to quantify POMP levels, which were normalized to KAS-6/1 WT cells arbitrarily set to 1.0. A representative autoradiograph from one of two independent experiments is shown. *E,* cells described in *D* were then exposed to bortezomib for 24 h at the indicated concentrations, and viability was determined with the tetrazolium reagent WST-1. Data presented are from three independently performed experiments and are presented as the mean ± S.D. (* $p < 0.05$ *versus* KAS-6/1 WT or OE-control). *F,* proteasome activity in the cells described in *D* was examined as described under "Experimental Procedures." Data are from three independent experiments and are presented as the mean ± S.D. (*, $p < 0.05$ *versus* KAS-6/1 WT or KAS-6/1 OE-control). *G,* OPM-2 bortezomib-resistant cells (OMP-2 V10R) were infected with lentiviral vectors expressing a scrambled sequence, non-targeting shRNA (*KO-NT*), or one of two different shRNAs targeting *POMP* (*KO-3* and *KO-5*). The success of *POMP* knockdown was verified with Western blotting and compared with β-actin as a loading control. Densitometry was performed to quantify POMP levels, which were normalized to OMP-2 V10R cells arbitrarily set to 1.0. A representative autoradiograph from one of two independent experiments is shown. *H,* cells described in *G* and OPM-2 drug-naive cells (*OPM-2 WT*) were then exposed to bortezomib for 24 h at the indicated concentrations, and viability was determined with the tetrazolium reagent WST-1. Data presented are from three independently performed experiments and are presented as the mean ± S.D. (*, $p < 0.05$ *versus* OPM-2 V10R or KO-NT). *I,* proteasome activity of the cells described in *G* was examined as described under "Experimental Procedures." Data are from three independent experiments and are presented as the mean ± S.D. (*, $p < 0.05$ *versus* OPM-2 V10R or OPM-2 V10R KO-NT). *J,* OPM-2 drug-naive cells (*OPM-2 WT*) were infected with lentiviral vectors without a cDNA insert (*OE-control*) or the cDNA for *POMP* (*OE-POMP*). The success of *POMP* overexpression was verified with Western blotting and compared with β-actin as a loading control. Densitometry was performed to quantify POMP levels, which were normalized to OPM-2 WT cells arbitrarily set to 1.0. A representative autoradiograph from one of two independent experiments is shown. *K,* cells described in *J* were then exposed to bortezomib for 24 h at the indicated concentrations, and viability was determined with the tetrazolium reagent WST-1. Data presented are from three independently performed experiments and are presented as the mean ± S.D. (*, $p < 0.05$ *versus* OPM-2 WT or OE-control). *L,* proteasome activity in the cells described in *J* was examined as under "Experimental Procedures." Data are from three independent experiments and are presented as the mean ± S.D. (*, $p <$ 0.05 *versus* OPM-2 WT or OPM-2 OE-control). *M,* KAS-6/1 cells with *POMP* overexpressed (*OE-POMP* cells) were transiently transfected with non-targeting shRNAs (*OE-shRNA-control*) or shRNAs targeting *POMP* (*OE-shRNA-POMP*). The cells and KAS-6/1 wild-type cells (*KAS-6/1 WT*) were then exposed to bortezomib for 24 h at the indicated concentrations, and viability was determined with the tetrazolium reagent WST-1. Data presented are from three independently performed experiments and are presented as the mean ± S.D. (*, $p < 0.05$ *versus* OE-POMP and OE-shRNA-control). *N,* OPM-2 cells with *POMP* overexpressed (*OE-POMP* cells) were transiently transfected with non-targeting shRNAs (*OE-shRNA-control*) or shRNAs targeting *POMP* (*OE-shRNA-POMP*). The cells and OPM-2 wild-type cells (*OPM-2 WT*) were then exposed to bortezomib for 24 h at the indicated concentrations, and viability was determined with the tetrazolium reagent WST-1. Data presented are from three independently performed experiments and are presented as the mean ± S.D. (*, $p < 0.05$ *versus* OE-POMP and OE-shRNA-control).

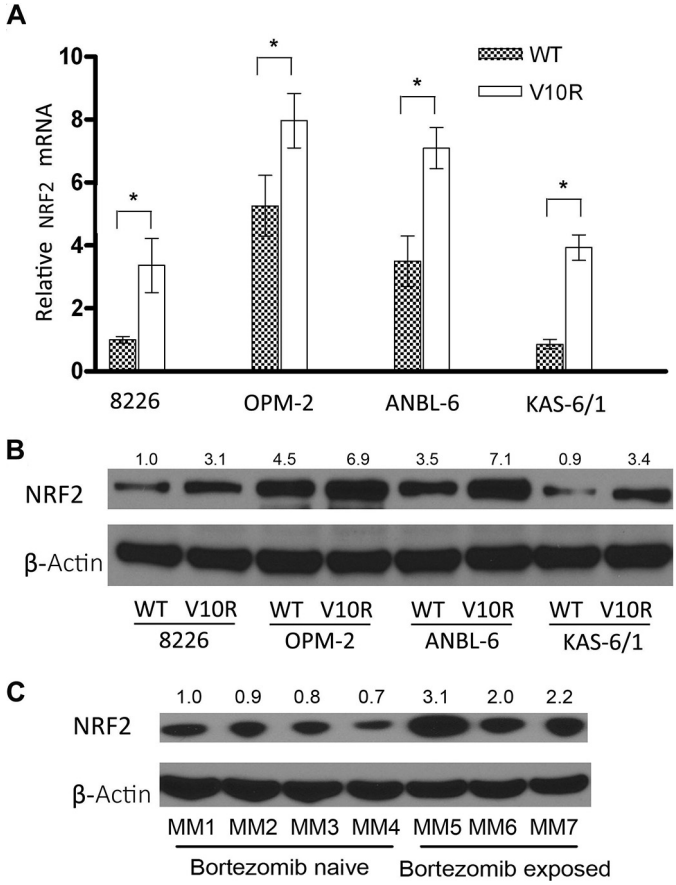

FIGURE 3. **Bortezomib resistance and *NRF2* levels in myeloma cell lines.** *A*, bortezomib-sensitive (*WT*) and bortezomib-resistant (*V10R*) myeloma cell lines, including RPMI 8226 (*8226*), OPM-2, ANBL-6, and KAS-6/1 cells, were subjected to qPCR to detect *NRF2* mRNA content, which was analyzed using the comparative C_T method and normalized to GAPDH as an internal control. *NRF2* expression in drug-naive 8226 cells was arbitrarily set at 1.0, and representative data are shown from one of three independent experiments along with the standard deviation (*, $p < 0.05$ *versus* WT). *B,* NRF2 protein levels were evaluated in these same cell lines by immunoblotting and compared with β-actin as a loading control. Densitometry was performed to quantify NRF2 levels, which were normalized to 8226 WT cells arbitrarily set to 1.0. A representative autoradiograph is shown from one of two independently performed experiments. *C,* NRF2 protein levels were evaluated in the primary myeloma cells by immunoblotting and compared with β-actin as a loading control. Densitometry was performed to quantify NRF2 levels, which were normalized to the MM1 sample arbitrarily set to 1.0. A representative autoradiograph is shown from one of two independently performed experiments.

son we had focused on *NRF2* as a target of interest among the many transcription factors that bound near the *POMP* promoter. To more directly test this possibility, we first performed ChIP in KAS-6/1 cells using either an anti-NRF2 antibody or control IgG, followed by PCR to detect sequences near the *POMP* promoter. Although nonspecific IgG did not appreciably precipitate such sequences, they were comparatively enriched when anti-NRF2 antibodies were used (Fig. 4*A*). Moreover, the enrichment was even greater in the KAS-6/1 V10R bortezomib-resistant cells, suggesting that there was greater binding of *NRF2*. Next, we used a biotin-labeled probe corresponding to one of the *NRF2* consensus sites and nuclear extract from KAS-6/1 V10R cells, which produced a strong protein-DNA complex in a mobility shift assay (Fig. 4*B*, *lane 2*) that could be competed with cold probe (Fig. 4*B*, *lane 3*). Finally, we prepared vectors containing either the *POMP* promoter upstream of a *Renilla* luciferase gene as a reporter (pPOMP-RenSP) or the thymidine kinase promoter upstream of a *Cypridina* luciferase reporter (pTK-Cluc), which was used as a transfection control. Compared with an empty vector *Renilla* luciferase reporter (Empty-RenSP; Fig. 4*C*, *1st bar*), transfection of the *POMP* reporter and an empty vector (pCMV6-XL5) revealed enhanced activity (Fig. 4*C*, *2nd bar*), consistent with a basal level of *POMP* activity in myeloma cells. Notably, when the *POMP* reporter was co-transfected with a vector expressing *NRF2* (pCMV6-XL5-NRF2), a substantial increase in *POMP* promoter activity was seen (Fig. 4*C*, *3rd bar*), consistent with an activating effect of NRF2 on the *POMP* promoter.

NRF2 Regulates Proteasome Activity—Our previous data suggested a direct role for the *NRF2/POMP* axis in proteasome activity, so to test that more directly, we developed KAS-6/1 V10R bortezomib-resistant cells in which *NRF2* was knocked down. Compared with WT or NT control cells, suppression of NRF2 with one of two different shRNAs reduced downstream *POMP* levels (Fig. 5*A*), and this was associated with a reduction in the chymotrypsin-like proteasome activity (Fig. 5*B*). When these cells were then treated with either vehicle or bortezomib, compared with the parental KAS-6/1 V10R and NT controls, the KO-6 and -8 cells with lower levels of NRF2 were consistently more sensitive to proteasome inhibition, and the level of bortezomib sensitivity almost reverted to that of KAS-6/1 WT cells (Fig. 5*C*). These findings were confirmed in OPM-2 bortezomib-resistant cells, where *NRF2* knockdown reduced *POMP* expression (Fig. 5*G*), proteasome activity (Fig. 5*H*), and cell viability (Fig. 5*I*). Conversely, when NRF2 was overexpressed in KAS-6/1 WT drug-naive cells, POMP expression also increased (Fig. 5*D*), as did proteasome activity (Fig. 5*E*), with up to a 5-fold or more induction, and cell viability (Fig. 5*F*). Finally, qualitatively comparable data were obtained when NRF2 was overexpressed in drug-naive OPM-2 cells (Fig. 5, *J–L*). Together, these data support the hypothesis that activation of the *NRF2/POMP* axis is associated with increased proteasome capacity, which could make myeloma cells more resistant to proteasome inhibition by reducing the imbalance between load and capacity.

Inhibition of NRF2 Sensitizes Bortezomib-resistant Cells—The involvement of *NRF2* in bortezomib resistance provided us with an avenue to suppress the *NRF2/POMP* pathway, because retinoic acid has been described to inhibit NRF2 activity through activation of retinoic acid receptor α (32). Because ATRA is a clinically relevant agent in this class, which is a standard of care for promyelocytic leukemia (33), we examined the possibility that it could be applied to bortezomib resistance. We exposed KAS-6/1 V10R cells to the indicated concentrations of ATRA, bortezomib, or both for 24 h, and we noted that bortezomib alone enhanced the levels of both NRF2 and POMP, although they decreased with exposure to ATRA alone. ATRA in combination with bortezomib also inhibited the levels of both NRF2 and POMP compared with single agent treatment with bortezomib (Fig. 6*A*). Notably, there was no associated change in the levels of KEAP1, which serves as an adaptor for the E3 ubiquitin ligase responsible for ubiquitination of NRF2 (34). Compared with the vehicle controls, the single agent ATRA or bortezomib treatments showed only a slight ability to

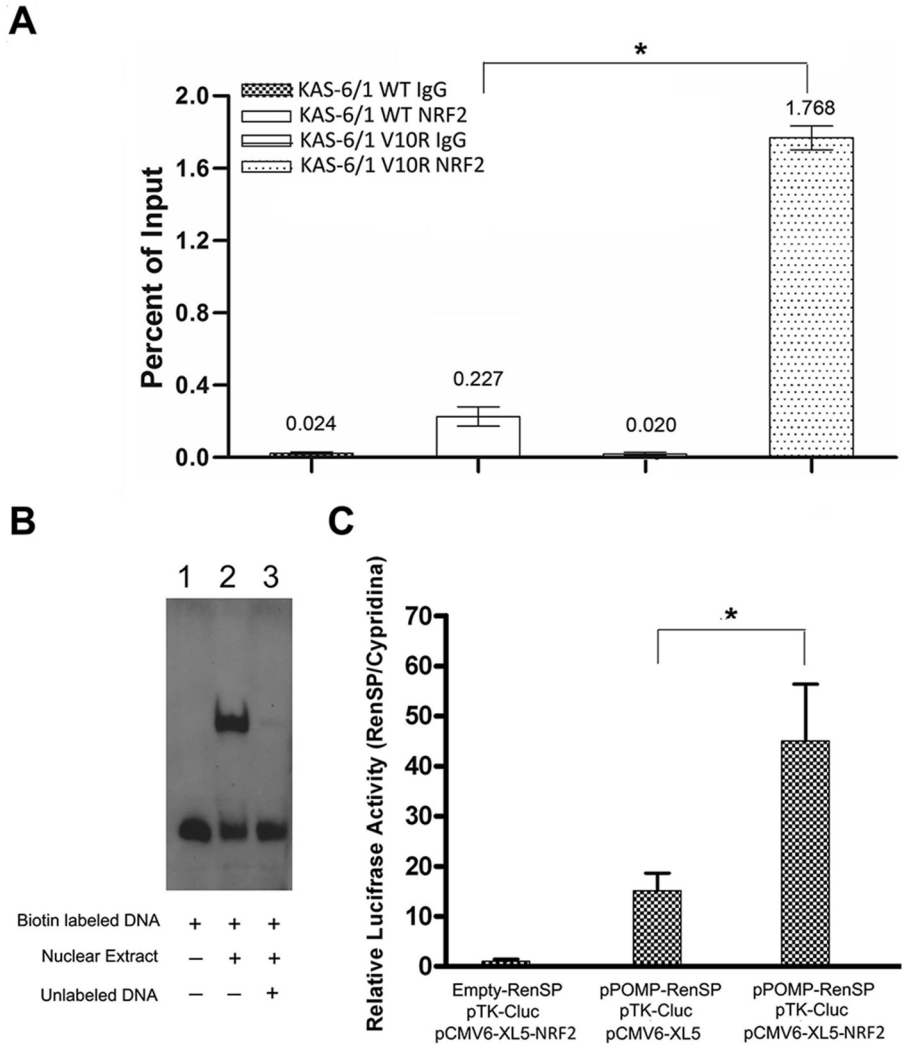

FIGURE 4. ***NRF2* and the *POMP* promoter.** *A,* chromatin immunoprecipitation assays were performed using either nonspecific immunoglobulins (*IgG*) or antibodies specific for *NRF2*. Primers described under "Experimental Procedures" were then used in quantitative real time PCR assays to detect the pulldown of sequences near the putative NRF2-binding site identified near the *POMP* promoter. The results were normalized to the input control, and all data are shown as the mean ± S.D. (*, $p < 0.01$) from three independently performed experiments. *B,* electrophoretic mobility shift assays were performed using an oligonucleotide representing one of the putative NRF2-binding sites from the *POMP* promoter. Binding reactions were prepared by incubating nuclear extracts with a biotin-labeled probe in the presence (+) or absence (−) of a 200-fold molar excess of specific DNA (unlabeled probe). Complexes were separated on 4% native polyacrylamide gels by electrophoresis, transferred to positively charged nylon membrane, and visualized using a streptavidin-horseradish peroxidase conjugate. *C,* luciferase reporter assays were used to examine the ability of NRF2 to activate the *POMP* promoter in KAS-6/1 cells. These were co-transfected in triplicate with constructs containing either no promoter with a *Renilla* luciferase promoter (*Empty-RenSP*) or a *POMP-Renilla* luciferase reporter (*pPOMP-RenSP*), along with a thymidine kinase promoter-*Cypridina* luciferase reporter (*pTK-Cluc*) as a transfection control. In addition, either an empty expression vector (*pCMV6-XL5*) or the same vector with the NRF2 cDNA (*pCMV6-XL5-NRF2*) was transfected. Luciferase activities were then measured, and *Renilla* luciferase activity was first normalized to the *Cypridina* luciferase activity. Then, the activity of the Empty-RenSP vector in cells transfected with pTK-Cluc and pCMV6-XL5-NRF2 was arbitrarily set at 1.0, and the activity elsewhere was normalized to this value (*, $p < 0.05$).

reduce the viability of KAS-6/1 V10R cells (Fig. 6*B*), but the combination regimens were much more effective in this regard. ATRA and bortezomib together produced a greater level of apoptosis, as measured by the appearance of the cleaved, activated form of caspase 3 (Fig. 6*C*), and the enhanced activity of the combinations was associated with a greater reduction in the chymotrypsin-like proteasome activity (Fig. 6*D*). Importantly, ATRA showed similar effects in OPM-2 bortezomib-resistant cells, where it reduced NRF2 and POMP levels (Fig. 6*E*), enhanced the ability of bortezomib to reduce cell viability (Fig. 6*F*), induced caspase cleavage (Fig. 6*G*), and suppressed proteasome activity (Fig. 6*H*).

To examine the possibility that ATRA could enhance the action of bortezomib in drug-sensitive cells, we performed comparable experiments in KAS-6/1 and OPM-2 WT cells. Similar trends were observed in KAS-6/1 (Fig. 6, *I–L*) and OPM-2 cells (Fig. 6, *M–P*), in that ATRA in combination with bortezomib inhibited the levels of both NRF2 and POMP compared with single agent treatment with bortezomib and enhanced cell death. However, the level of enhanced cell death was smaller than that in the BR cells, in part because, as expected, bortezomib alone produced a much more dramatic effect.

ATRA Enhances Bortezomib Activity against Primary Samples and in Vivo—To contribute to the design of future clinical trials, we next examined the possibility that ATRA could enhance the efficacy of bortezomib against $CD138^+$ primary plasma cells from patients with multiple myeloma. In samples

where bortezomib showed minimal activity, as defined by a less than 20% reduction in viability as a single agent, such as in MM8 and MM9 (Fig. 7*A*), addition of ATRA, which itself showed even less efficacy, showed an enhanced reduction in viability with the combination. The same was true in samples where bortezomib showed greater activity, such as MM10 through MM12, where again ATRA increased the ability of bortezomib to reduce viability. Finally, it was also of interest to validate these findings *in vivo* using a bortezomib-resistant xenograft model. Seven days after inoculation of KAS-6/1 V10R cells, subject mice were randomized to treatment with intraperitoneal injections of vehicle, bortezomib, ATRA, or the combination, and tumor volumes were determined from measurements performed by an investigator blinded to the treatment assignments. Bortezomib and ATRA alone did show some activity in this setting, but the bortezomib and ATRA combination regimen reduced tumor volume (Fig. 7*B*) compared with either agent alone. These differences reached statistical significance

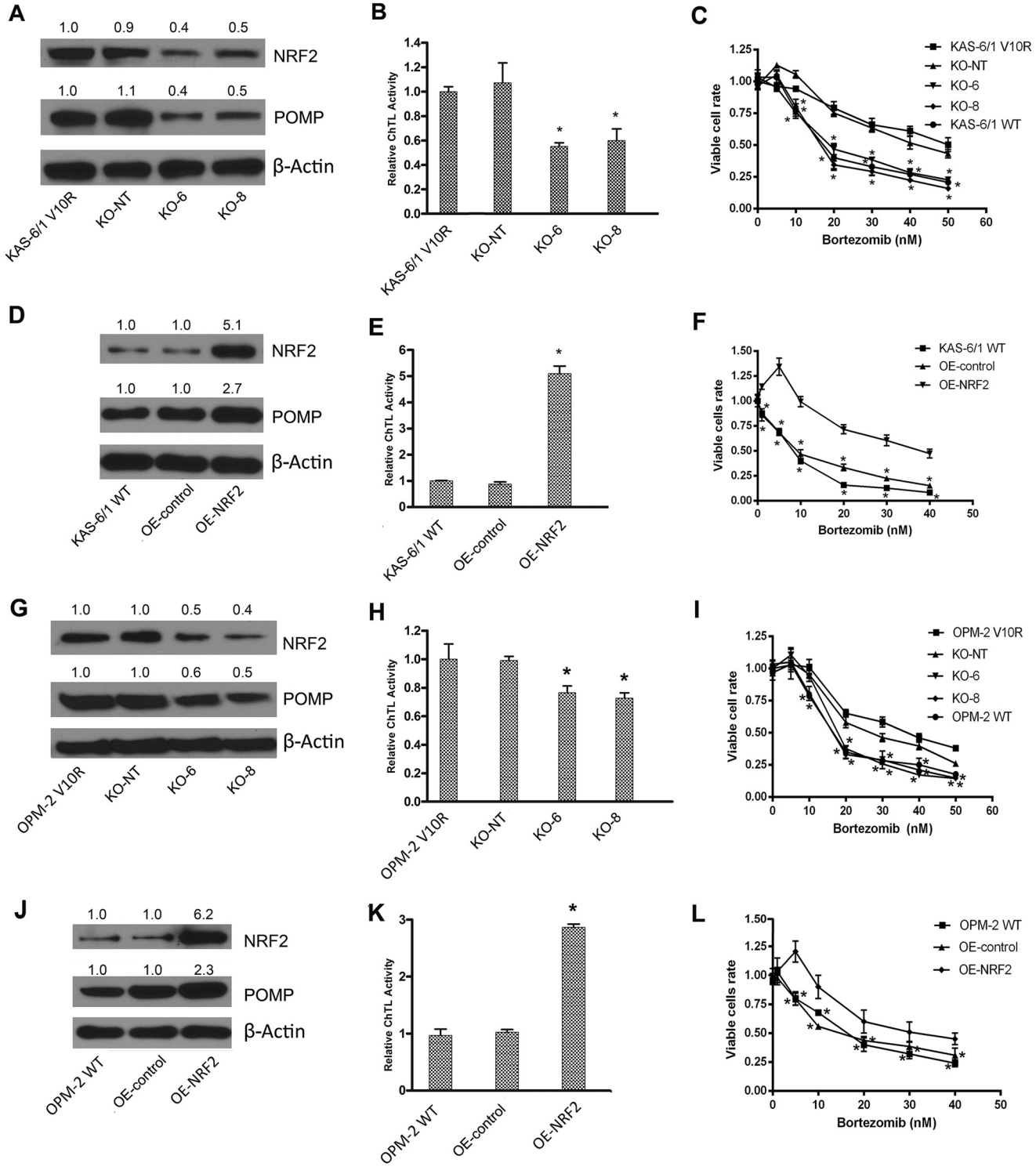

(Fig. 7*C*), supporting the possibility that this approach could be translated to the clinic to overcome bortezomib resistance. We next tested whether treatment with bortezomib and ATRA changed the expression of *POMP* or the 20S proteasome *β5* subunit targeted by bortezomib expression at day 32. ATRA alone inhibited the mRNA levels of both *POMP* (Fig. 7*D*, *left panel*) and the *β5* proteasome subunit (PSMB5; Fig. 7*D*, *right panel*) compared with the vehicle controls, whereas bortezomib alone stimulated expression of these two genes. In contrast, the addition of ATRA to bortezomib significantly reduced *POMP* and *β5* expression compared with bortezomib alone, and these returned to levels comparable with those seen in vehicle-treated controls. Finally, both *POMP* and *β5* expression at the protein level changed in a pattern consistent with that of their mRNAs (Fig. 7*E*).

Discussion

The proteasome inhibitor bortezomib is an important part of the standard of care for myeloma patients (1–7), and carfilzomib, a second generation irreversible inhibitor, has recently been approved in the relapsed and refractory setting (35). Following the lead of bortezomib, carfilzomib is being further developed as part of rationally designed regimens for patients with either relapsed disease (36, 37) or newly diagnosed myeloma (38). Moreover, proteasome inhibitors with novel properties are being developed, such as marizomib, which may inhibit all three of the major proteolytic activities of the proteasome, as well as orally bioavailable inhibitors, including ixazomib and oprozomib (39). In this light, and considering the contribution of this class of drugs to the improving outcomes in myeloma (9–12), it seems reasonable to expect that they will remain part of the standard of care for this disease for many years to come. However, due perhaps in part to their incorporation into the treatment of newly diagnosed patients, resistance to proteasome inhibitors is an emerging clinical problem, especially because such patients have a poor prognosis. Indeed, bortezomib-refractory patients who were also relapsed following, refractory to, or ineligible to receive immunomodulatory agents have been reported to have a median survival of less than 1 year (40). This indicates a strong need to better understand the mechanisms underlying bortezomib resistance because this could lead to the design of regimens to overcome this phenotype, which would extend the utility of these drugs and, more importantly, if validated, prolong patient survival.

This study has identified *POMP* as a modulator of bortezomib resistance in myeloma, because its overexpression was seen in resistant cell lines and primary samples (Fig. 1). *POMP* suppression with shRNAs restored sensitivity, although its overexpression in drug-naive cells was sufficient to induce resistance (Fig. 2). Also, starting with the observation that *NRF2* was induced in bortezomib-resistant cells as well (Fig. 3), we have documented that NRF2 controls POMP levels in myeloma through an impact on transcription from the *POMP* promoter (Fig. 4). Notably, overexpression or suppression of either POMP (Fig. 2) or NRF2 (Fig. 5) had a consistently greater differential impact on bortezomib sensitivity in KAS-6/1 cells than it did in OPM-2 cells. Interestingly, OPM-2 cells expressed higher basal levels of both *POMP* and *NRF2*, and this may explain the differential effects in these cell lines. A high basal level of *POMP* and *NRF2* could blunt the impact of a further overexpression, although a fixed reduction of either would leave higher levels in OPM-2 cells than in KAS-6/1 cells, thereby blunting the impact of shRNAs. These findings are consistent with a recent study that linked activation of NRF2 by *tert*-butylhydroquinone and other approaches to increased *POMP* expression and pluripotency in human embryonic stem cells (41). Moreover, antioxidants and oxidative stress have

FIGURE 5. ***NRF2, POMP*, and proteasome activity.** *A,* KAS-6/1 bortezomib-resistant cells were transfected with lentiviral vectors expressing a scrambled sequence, non-targeting shRNA (*KO-NT*), or one of two different shRNAs targeting and suppressing *NRF2* (*KO-6* and *KO-8*). Knockdown of *NRF2*, and its impact on downstream POMP, was examined by Western blotting and compared with *β*-actin as a loading control. Densitometry was performed to quantify NRF2 and POMP levels, which were normalized to KAS-6/1 V10R cells arbitrarily set to 1.0. A representative autoradiograph from one of two independent experiments is shown. *B,* proteasome activity of the cells described in *A* was examined as detailed under "Experimental Procedures." Data are from three independent experiments and are presented as the mean ± S.D. (*, $p < 0.05$ *versus* KAS-6/1 V10R or KAS-6/1 V10R KO-NT). *C,* cells described in *A* and KAS-6/1 bortezomib-sensitive (KAS-6/1 WT) cells were then exposed to bortezomib for 24 h at the indicated concentrations, and viability was determined with the tetrazolium reagent WST-1. Data presented are from three independently performed experiments and are presented as the mean ± S.D. (*, $p < 0.05$ *versus* KAS-6/1 V10R or KO-NT). *D,* KAS-6/1 bortezomib-sensitive (*KAS-6/1 WT*) cells were transfected with control lentiviral vectors (*KAS-6/1 OE-control)* or lentiviral vectors containing the *NRF2* cDNA (*KAS-6/1 OE-NRF2*). Expression of NRF2 and POMP was examined with Western blotting and compared with *β*-actin as a loading control. Densitometry was performed to quantify NRF2 and POMP levels, which were normalized to KAS-6/1 WT cells arbitrarily set to 1.0. A representative autoradiograph from one of two independent experiments is shown. *E,* proteasome activity in the cells described in *D* was examined as under "Experimental Procedures." Data are from three independent experiments and are presented as the mean ± S.D. (*, $p < 0.05$ *versus* KAS-6/1 WT or KAS-6/1 OE-control). *F,* cells described in *D* were then exposed to bortezomib for 24 h at the indicated concentrations, and viability was determined with the tetrazolium reagent WST-1. Data presented are from three independently performed experiments and are presented as the mean ± S.D. (*, $p < 0.05$ *versus* KAS-6/1 OE-NRF2). *G,* OPM-2 bortezomib-resistant cells were transfected with lentiviral vectors expressing a scrambled sequence, non-targeting shRNA (*KO-NT*), or one of two different shRNAs targeting and suppressing *NRF2* (*KO-6* and *KO-8*). Knockdown of *NRF2*, and its impact on downstream POMP, was examined by Western blotting and compared with *β*-actin as a loading control. Densitometry was performed to quantify NRF2 and POMP levels, which were normalized to OPM-2 V10R cells arbitrarily set to 1.0. A representative autoradiograph from one of two independent experiments is shown. *H,* proteasome activity of the cells described in *G* was examined as described under "Experimental Procedures." Data are from three independent experiments and are presented as the mean ± S.D. (*, $p < 0.05$ *versus* OPM-2 V10R or OPM-2 V10R KO-NT). *I,* cells described in *G* and OPM-2 bortezomib-sensitive (*OPM-2 WT*) cells were then exposed to bortezomib for 24 h at the indicated concentrations, and viability was determined with the tetrazolium reagent WST-1. Data presented are from three independently performed experiments and are presented as the mean ± S.D. (*, $p < 0.05$ *versus* OPM-2 V10R or KO-NT). *J,* OPM-2 bortezomib-sensitive (*OPM-2 WT*) cells were transfected with control lentiviral vectors (*OPM-2 OE-control*) or lentiviral vectors containing the *NRF2* cDNA (*OPM-2 OE-NRF2*). Expression of NRF2 and POMP was examined with Western blotting and compared with *β*-actin as a loading control. Densitometry was performed to quantify NRF2 and POMP levels, which were normalized to OPM-2 WT cells arbitrarily set to 1.0. A representative autoradiograph from one of two independent experiments is shown. *K,* proteasome activity in the cells described in *J* was examined as under "Experimental Procedures." Data are from three independent experiments and are presented as the mean ± S.D. (*, $p < 0.05$ *versus* OPM-2 WT or OPM-2 OE-control). *L,* cells described in *J* were then exposed to bortezomib for 24 h at the indicated concentrations, and viability was determined with the tetrazolium reagent WST-1. Data presented are from three independently performed experiments and are presented as the mean ± S.D. (*, $p < 0.05$ *versus* OPM-2 OE-NRF2).

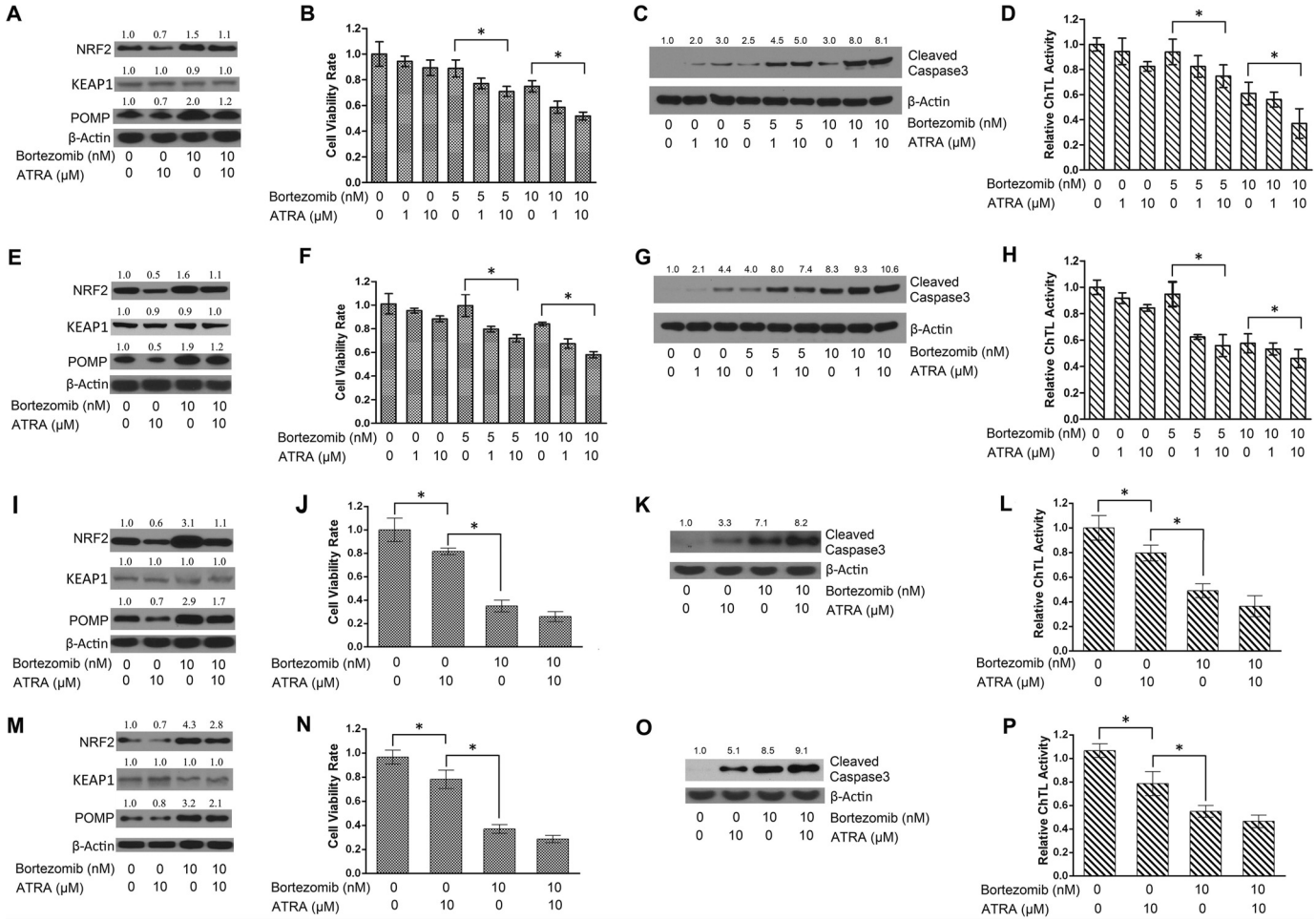

FIGURE 6. **ATRA and bortezomib sensitivity.** *A,* KAS-6/1 bortezomib-resistant cells (KAS-6/1 V10R) were exposed to the indicated concentrations of ATRA, bortezomib, or both for 24 h, and expression of NRF2, KEAP1, and POMP was examined by Western blotting, all relative to β-actin as a loading control. A representative autoradiograph from one of two independent experiments is shown. Densitometry was performed to quantify NRF2, KEAP1, and POMP levels, which were normalized to the vehicle control arbitrarily set to 1.0. *B,* KAS-6/1 bortezomib-resistant cells were treated with the indicated concentrations of ATRA, bortezomib, or both for 24 h. Cellular viability measurements were then performed using the WST-1 assay as described under "Experimental Procedures." All data points were normalized to the vehicle control, which was arbitrarily set at 100% viability. Mean viability values are provided from three independently performed experiments ± S.D., and the Student's paired *t* test was used to determine statistical significance (*, $p < 0.05$). *C,* levels of apoptosis were determined in cells treated as described in *B* by Western blotting to detect the cleaved fragment of caspase 3, with β-actin as a loading control. A representative autoradiograph from one of two independent experiments is shown. Densitometry was performed to quantify the cleaved caspase 3 level, which was normalized to the vehicle control arbitrarily set to 1.0. *D,* proteasome chymotrypsin-like activity was measured as described under "Experimental Procedures" in cells treated as above. All data points were normalized to the vehicle control, which was arbitrarily set at 100% activity. Mean proteasome activity values are provided from three independent experiments ± S.D., and the Student's paired *t* test was used to determine statistical significance (*, $p <$ 0.05). KAS-6/1 bortezomib-sensitive cells (KAS-6/1 WT) were exposed to the indicated concentrations of ATRA, bortezomib, or both for 24 h. Abundance of NRF2, KEAP1, and POMP, cellular viability, and abundance of cleaved caspase 3 and proteasome chymotrypsin-like activity are shown in *I–L*, respectively. *E,* OPM-2 bortezomib-resistant cells (OPM-2 V10R) were exposed to the indicated concentrations of ATRA, bortezomib, or both for 24 h, and expression of NRF2, KEAP1, and POMP was tested by Western blotting, all relative to β-actin as a loading control. A representative autoradiograph from one of two independent experiments is shown. Densitometry was performed to quantify NRF2, KEAP1, and POMP levels, which were normalized to the vehicle control arbitrarily set to 1.0. *F,* OPM-2 bortezomib-resistant cells were treated with the indicated concentrations of ATRA, bortezomib, or both for 24 h. Cellular viability measurements were then performed using the WST-1 assay as described under "Experimental Procedures." All data points were normalized to the vehicle control, which was arbitrarily set at 100% viability. Mean viability values are provided from three independently performed experiments ± S.D., and the Student's paired *t* test was used to determine statistical significance (*, $p < 0.05$). *G,* levels of apoptosis were determined in cells treated as described in *F* by Western blotting to detect the cleaved fragment of caspase 3, with β-actin as a loading control. A representative autoradiograph from one of two independent experiments is shown. Densitometry was performed to quantify the cleaved caspase 3 levels, which were normalized to the vehicle control arbitrarily set to 1.0. *H,* proteasome chymotrypsin-like activity was measured as described under "Experimental Procedures" in cells treated as above. All data points were normalized to the vehicle control, which was arbitrarily set at 100% activity. Mean proteasome activity values are provided from three independent experiments ± S.D., and the Student's paired *t* test was used to determine statistical significance (*, $p < 0.05$). OPM-2 bortezomib-sensitive cells (OPM-2 WT) were exposed to the indicated concentrations of ATRA, bortezomib, or both for 24 h. Expression of NRF2, KEAP1, and POMP, cellular viability, expression of cleaved caspase 3, and proteasome chymotrypsin-like activity are shown in *M–P*, respectively.

been shown to enhance proteasome subunit expression through signaling pathways involving NRF2 (42, 43). However, because overexpression of *POMP* was by itself sufficient to induce bortezomib resistance in drug-naive cells (Fig. 2), this suggests that the compendium of *NRF2*-regulated genes was not required for this phenotype and that *POMP* may be rate-limiting. In addition, this observation is especially interesting because *NRF1* was previously implicated in the recovery of mammalian cells from proteasome inhibition by up-regulating proteasome subunit expression (44). Together, these findings

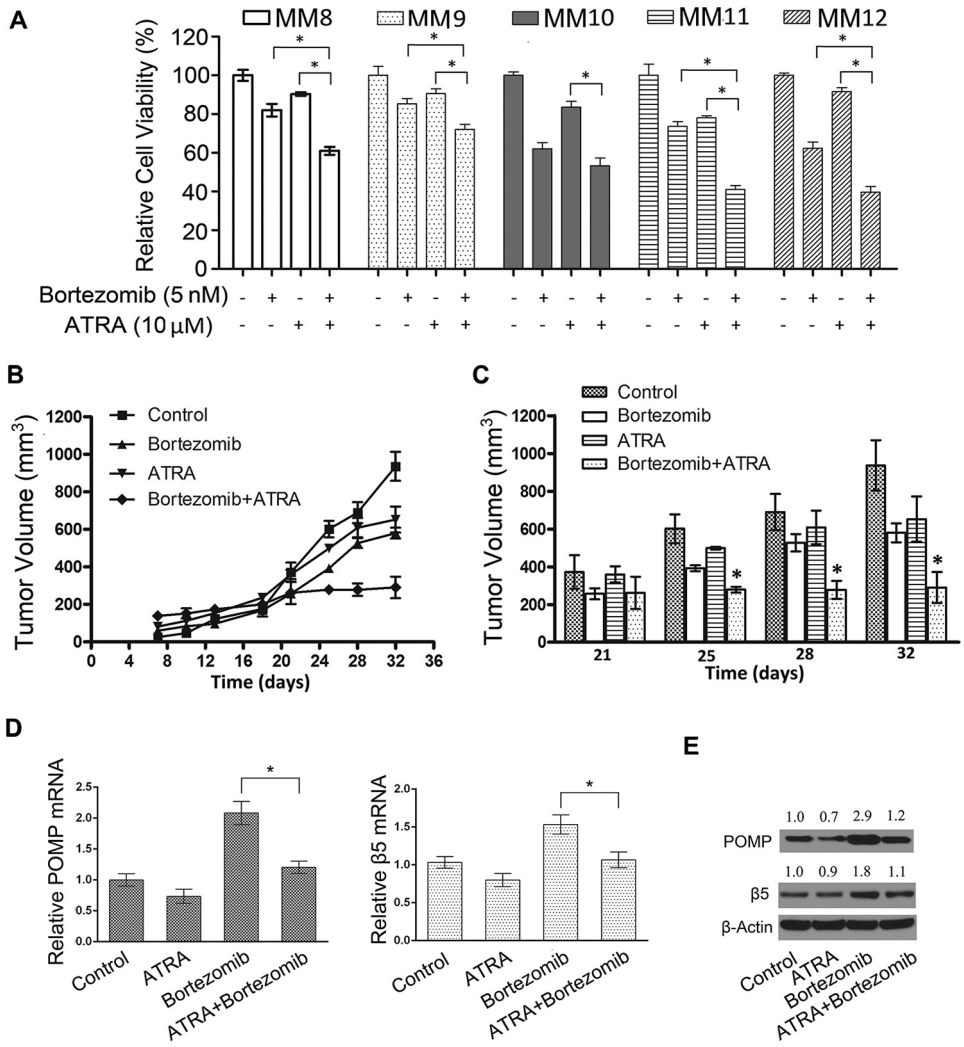

FIGURE 7. **Efficacy of ATRA and bortezomib against primary cells and *in vivo*.** *A,* purified CD138$^+$ plasma cells obtained from patients with myeloma were treated for 48 h with vehicle, bortezomib, ATRA, or the combination at the indicated concentrations, and viability was then analyzed using the WST-1 assay. All values were normalized to the vehicle control, which was set arbitrarily at 100%, and presented as the average of triplicate measurements on the same day ± S.D. (*, $p < 0.05$). *B,* immunodeficient mice were subcutaneously implanted with bortezomib-resistant KAS-6/1 cells and after 7 days were randomized to treatment with either vehicle, bortezomib (0.5 mg/kg), ATRA (40 mg/kg), or the combination, with treatment given three times weekly via intraperitoneal injections. Tumor growth was monitored by caliper measurement and calculated as the tumor volume using the equation ($0.4 \times l \times w^2$). Standard deviation is shown for each time point from a cohort of five mice in each treatment group. *C,* measured tumor volumes from mouse xenografts from day 21 to day 32 of the experiment described in *B* are shown in greater detail. Statistically significant values are determined by the conditional χ^2 test and indicated by *, which denotes $p < 0.05$ *versus* vehicle, bortezomib, or ATRA. *D,* quantitative PCR analysis was performed to determine *POMP* and *β5* levels in xenograft tumors treated with vehicle, bortezomib, ATRA, or the combination. *E,* POMP and *β5* levels in xenograft tumors were determined by immunoblotting. Densitometry was performed to quantify POMP and *β5* levels, which were normalized to the control arbitrarily set to 1.0 (*, $p < 0.05$).

suggest that *NRF1* and *NRF2* may work in a coordinated fashion, with the former inducing proteasome subunits and the latter enhancing proteasome assembly, both of which would be needed to restore full proteasome function. Because knockdown of *NRF2* reduced proteasome activity, and its overexpression enhanced proteasome capacity (Fig. 5), we then studied the *NRF2* inhibitor ATRA, which sensitized resistant cells to bortezomib, and also to some extent enhanced bortezomib efficacy in sensitive cells, although to a much lesser extent (Fig. 6). The lesser impact of ATRA in sensitive cells was expected, as bortezomib shows strong activity against drug-naive myeloma models, and baseline levels of *POMP* in sensitive cells are lower (Fig. 1). Notably, ATRA consistently reduced levels of both *NRF2* and *POMP* in bortezomib-naive and -resistant cells either alone or in combination with bortezomib. Our finding of increased activation of *NRF2* is consistent with the data of Stessman *et al.* (45), who found in mouse and human cell line models of myeloma that bortezomib resistance produced a gene signature enriched for downstream targets of this transcription factor, although they did not look at what downstream *NRF2* effectors could be involved.

ATRA with bortezomib enhanced activity against primary plasma cells and, in our *in vivo* studies, against a murine model of bortezomib resistance (Fig. 7). We used a subcutaneous xenograft model in these studies, which probably best represents myeloma with an extramedullary plasmacytoma. This has been associated with a poor clinical prognosis in myeloma patients (46) and may be linked to bortezomib resistance (47), but it does not fully recapitulate a physiologically relevant bone marrow microenvironment. Thus, studies in a systemic

myeloma model or a humanized model providing bone cells, immune cells, and the appropriate cytokine milieu (48) could provide further insights into the utility of ATRA as an approach to resensitize to bortezomib. In our *in vivo* modeling, ATRA reduced *POMP* mRNA and protein levels, which was expected based on its impact on the *NRF2-POMP* axis. Also of interest was that β*5* subunit protein and mRNA expression levels were suppressed by ATRA. The reduction of β5 protein could be due to the short half-life of the β5 precursor (49), whose turnover could be enhanced when it cannot be incorporated into proteasomes because of reduced POMP levels. Alternatively, or in addition to that, ATRA may have a direct effect on the *PSMB5* gene to reduce promoter transcription and thereby protein levels, which would provide another mechanism for it to enhance the activity of bortezomib. Additional studies will therefore be needed to fully elucidate the effects of ATRA on proteasome biogenesis pathways. However, because inhibition of *NRF2* and *POMP* using shRNAs was sufficient to enhance the efficacy of bortezomib, at least part of ATRA's sensitization likely is due to its effect on the *NRF2/POMP* axis.

POMP is a proteasome assembly chaperone that is involved in the addition of subunits to a pre-formed ring of seven subunits (50) and generates a hemi-proteasome once the β ring assembly is completed. Two of these hemi-proteasomes are then combined to form the 20S core particle, which contains all of the proteolytic activities of the proteasome (21, 22). In addition, POMP can bind to endoplasmic reticulum membranes to facilitate proteasome assembly close to one of the major sites at which proteasomes function (51), but POMP is ultimately cleaved by the proteasome once the latter is activated (21, 22). A number of studies have previously shown that transient inhibition of the proteasome produces up-regulation of proteasome subunit synthesis (52, 53), as cells attempt to restore normal protein homeostasis. POMP is also up-regulated under such conditions, but it has not been completely clear whether this was due to coordinate regulation of POMP with proteasome subunits or whether this was simply because POMP degradation was suppressed by proteasome inhibition. Our data show that *POMP* overexpression can be a genetically stable, acquired phenotype in proteasome inhibitor resistance, because these cells were free of bortezomib treatment for as long as 8 weeks or more. Also, in that *POMP* overexpression or suppression was by itself sufficient to confer resistance or sensitization to bortezomib, respectively, our findings indicate that *POMP* alone, aside from any impact on *NRF2*, is a mediator of bortezomib sensitivity. Thus, our cell lines may serve to some extent as models of what is seen clinically, because retreatment with bortezomib, even in patients who had all previously responded well to this agent, produces response rates of only 50–60% (54, 55), indicating a rapid acquisition of resistance. Moreover, the involvement of *POMP* may provide some indication of why these patients have a poor overall prognosis, because both *NRF2* (56) and *POMP* (30) have been linked to cellular defense mechanisms against electrophilic and oxidative stress. In that other drugs used against myeloma work in part by generating reactive oxygen species, including alkylating agents and anthracyclines, activation of the *NRF2/POMP* axis may reduce sensitivity to these other drug classes as well.

Finally, our translational studies suggest that strategies targeting and suppressing the *NRF2/POMP* axis may be attractive ones to enhance bortezomib sensitivity in drug-naive patients and to restore some sensitivity in drug-resistant patients. Approaches that should be successful in this regard include the use of *NRF2* inhibitors or of agents that would induce *KEAP1*, which would contribute to turnover of *NRF2* (57) and thereby reduce POMP levels. In this work, we have validated ATRA as one such strategy, and this is clinically relevant, because ATRA is already in use against acute promyelocytic leukemia (33). A regimen of ATRA with bortezomib could therefore be piloted first in phase I to determine its safety and then to examine its ability to overcome resistance to this proteasome inhibitor in larger and preferably randomized phase II or III studies.

Author Contributions—B. L. designed and performed the majority of the experiments, analyzed the data, prepared the figures, and wrote a draft of the manuscript. J. F. facilitated access to primary samples. J. F., P. C., X. G., and Y. L. assisted with some experiments and were involved in data analysis and manuscript preparation and provided statistical analyses of mouse xenograft modeling. I. K., H. W., and X. D.-Z. performed *in vivo* experiments. H. W. generated lentiviral constructs. R. Z. O. provided research guidance, supervised the work herein, and proofed the manuscript.

References

1. Richardson, P. G., Barlogie, B., Berenson, J., Singhal, S., Jagannath, S., Irwin, D., Rajkumar, S. V., Srkalovic, G., Alsina, M., Alexanian, R., Siegel, D., Orlowski, R. Z., Kuter, D., Limentani, S. A., Lee, S., *et al.* (2003) A phase 2 study of bortezomib in relapsed, refractory myeloma. *N. Engl. J. Med.* **348,** 2609–2617
2. Richardson, P. G., Sonneveld, P., Schuster, M. W., Irwin, D., Stadtmauer, E. A., Facon, T., Harousseau, J. L., Ben-Yehuda, D., Lonial, S., Goldschmidt, H., Reece, D., San-Miguel, J. F., Bladé, J., Boccadoro, M., Cavenagh, J., *et al.* (2005) Bortezomib or high-dose dexamethasone for relapsed multiple myeloma. *N. Engl. J. Med.* **352,** 2487–2498
3. Orlowski, R. Z., Nagler, A., Sonneveld, P., Bladé, J., Hajek, R., Spencer, A., San Miguel, J., Robak, T., Dmoszynska, A., Horvath, N., Spicka, I., Sutherland, H. J., Suvorov, A. N., Zhuang, S. H., Parekh, T., *et al.* (2007) Randomized phase III study of pegylated liposomal doxorubicin plus bortezomib compared with bortezomib alone in relapsed or refractory multiple myeloma: combination therapy improves time to progression. *J. Clin. Oncol.* **25,** 3892–3901
4. San Miguel, J. F., Schlag, R., Khuageva, N. K., Dimopoulos, M. A., Shpilberg, O., Kropff, M., Spicka, I., Petrucci, M. T., Palumbo, A., Samoilova, O. S., Dmoszynska, A., Abdulkadyrov, K. M., Schots, R., Jiang, B., Mateos, M. V., *et al.* (2008) Bortezomib plus melphalan and prednisone for initial treatment of multiple myeloma. *N. Engl. J. Med.* **359,** 906–917
5. Harousseau, J. L., Attal, M., Avet-Loiseau, H., Marit, G., Caillot, D., Mohty, M., Lenain, P., Hulin, C., Facon, T., Casassus, P., Michallet, M., Maisonneuve, H., Benboubker, L., Maloisel, F., Petillon, M. O., *et al.* (2010) Bortezomib plus dexamethasone is superior to vincristine plus doxorubicin plus dexamethasone as induction treatment prior to autologous stem-cell transplantation in newly diagnosed multiple myeloma: results of the IFM 2005–01 phase III trial. *J. Clin. Oncol.* **28,** 4621–4629
6. Cavo, M., Tacchetti, P., Patriarca, F., Petrucci, M. T., Pantani, L., Galli, M., Di Raimondo, F., Crippa, C., Zamagni, E., Palumbo, A., Offidani, M., Corradini, P., Narni, F., Spadano, A., Pescosta, N., *et al.* (2010) Bortezomib with thalidomide plus dexamethasone compared with thalidomide plus dexamethasone as induction therapy before, and consolidation therapy after, double autologous stem-cell transplantation in newly diagnosed multiple myeloma: a randomised phase 3 study. *Lancet* **376,** 2075–2085
7. Sonneveld, P., Schmidt-Wolf, I. G., van der Holt, B., El Jarari, L., Bertsch,

U., Salwender, H., Zweegman, S., Vellenga, E., Broyl, A., Blau, I. W., Weisel, K. C., Wittebol, S., Bos, G. M., Stevens-Kroef, M., Scheid, C., *et al.* (2012) Bortezomib induction and maintenance treatment in patients with newly diagnosed multiple myeloma: results of the randomized phase III HOVON-65/GMMG-HD4 trial. *J. Clin. Oncol.* **30,** 2946–2955
8. Anderson, K. C., Alsina, M., Bensinger, W., Biermann, J. S., Cohen, A. D., Devine, S., Djulbegovic, B., Faber, E. A., Jr., Gasparetto, C., Hernandez-Illizaliturri, F., Huff, C. A., Kassim, A., Krishnan, A. Y., Liedtke, M., Meredith, R., *et al.* (2013) Multiple myeloma, version 1.2013. *J. Natl. Compr. Canc. Netw.* **11,** 11–17
9. Mahindra, A., Laubach, J., Raje, N., Munshi, N., Richardson, P. G., and Anderson, K. (2012) Latest advances and current challenges in the treatment of multiple myeloma. *Nat. Rev. Clin. Oncol.* **9,** 135–143
10. Pozzi, S., Marcheselli, L., Bari, A., Liardo, E. V., Marcheselli, R., Luminari, S., Quaresima, M., Cirilli, C., Ferri, P., Federico, M., and Sacchi, S. (2013) Survival of multiple myeloma patients in the era of novel therapies confirms the improvement in patients younger than 75 years: a population-based analysis. *Br. J. Haematol.* **163,** 40–46
11. Kumar, S. K., Dispenzieri, A., Lacy, M. Q., Gertz, M. A., Buadi, F. K., Pandey, S., Kapoor, P., Dingli, D., Hayman, S. R., Leung, N., Lust, J., McCurdy, A., Russell, S. J., Zeldenrust, S. R., Kyle, R. A., and Rajkumar, S. V. (2014) Continued improvement in survival in multiple myeloma: changes in early mortality and outcomes in older patients. *Leukemia* **28,** 1122–1128
12. Ozaki, S., Harada, T., Saitoh, T., Shimazaki, C., Itagaki, M., Asaoku, H., Kuroda, Y., Chou, T., Yoshiki, Y., Suzuki, K., Murakami, H., Hayashi, K., Mina, R., Palumbo, A., and Shimizu, K. (2014) Survival of multiple myeloma patients aged 65–70 years in the era of novel agents and autologous stem cell transplantation. A multicenter retrospective collaborative study of the Japanese Society of Myeloma and the European Myeloma Network. *Acta Haematol.* **132,** 211–219
13. Cenci, S., Mezghrani, A., Cascio, P., Bianchi, G., Cerruti, F., Fra, A., Lelouard, H., Masciarelli, S., Mattioli, L., Oliva, L., Orsi, A., Pasqualetto, E., Pierre, P., Ruffato, E., Tagliavacca, L., and Sitia, R. (2006) Progressively impaired proteasomal capacity during terminal plasma cell differentiation. *EMBO J.* **25,** 1104–1113
14. Bianchi, G., Oliva, L., Cascio, P., Pengo, N., Fontana, F., Cerruti, F., Orsi, A., Pasqualetto, E., Mezghrani, A., Calbi, V., Palladini, G., Giuliani, N., Anderson, K. C., Sitia, R., and Cenci, S. (2009) The proteasome load *versus* capacity balance determines apoptotic sensitivity of multiple myeloma cells to proteasome inhibition. *Blood* **113,** 3040–3049
15. Chen, D., Frezza, M., Schmitt, S., Kanwar, J., and Dou, Q. P. (2011) Bortezomib as the first proteasome inhibitor anticancer drug: current status and future perspectives. *Curr. Cancer Drug Targets* **11,** 239–253
16. Laubach, J. P., Mitsiades, C. S., Roccaro, A. M., Ghobrial, I. M., Anderson, K. C., and Richardson, P. G. (2009) Clinical challenges associated with bortezomib therapy in multiple myeloma and Waldenstroms macroglobulinemia. *Leukemia Lymphoma* **50,** 694–702
17. Orlowski, R. Z., and Kuhn, D. J. (2008) Proteasome inhibitors in cancer therapy: lessons from the first decade. *Clin. Cancer Res.* **14,** 1649–1657
18. Lü, S., Yang, J., Song, X., Gong, S., Zhou, H., Guo, L., Song, N., Bao, X., Chen, P., and Wang, J. (2008) Point mutation of the proteasome β5 subunit gene is an important mechanism of bortezomib resistance in bortezomib-selected variants of Jurkat T cell lymphoblastic lymphoma/leukemia line. *J. Pharmacol. Exp. Ther.* **326,** 423–431
19. Lü, S., Chen, Z., Yang, J., Chen, L., Zhou, H., Xu, X., Li, J., Han, F., and Wang, J. (2010) The effects of proteasome inhibitor bortezomib on a P-gp positive leukemia cell line K562/A02. *Int. J. Lab. Hematol.* **32,** e123–31
20. Oerlemans, R., Franke, N. E., Assaraf, Y. G., Cloos, J., van Zantwijk, I., Berkers, C. R., Scheffer, G. L., Debipersad, K., Vojtekova, K., Lemos, C., van der Heijden, J. W., Ylstra, B., Peters, G. J., Kaspers, G. L., Dijkmans, B. A., *et al.* (2008) Molecular basis of bortezomib resistance: proteasome subunit β5 (PSMB5) gene mutation and overexpression of PSMB5 protein. *Blood* **112,** 2489–2499
21. Marques, A. J., Palanimurugan, R., Matias, A. C., Ramos, P. C., and Dohmen, R. J. (2009) Catalytic mechanism and assembly of the proteasome. *Chem. Rev.* **109,** 1509–1536
22. Murata, S., Yashiroda, H., and Tanaka, K. (2009) Molecular mechanisms of proteasome assembly. *Nat. Rev. Mol. Cell Biol.* **10,** 104–115
23. Politou, M., Karadimitris, A., Terpos, E., Kotsianidis, I., Apperley, J. F., and Rahemtulla, A. (2006) No evidence of mutations of the PSMB5 (β-5 subunit of proteasome) in a case of myeloma with clinical resistance to bortezomib. *Leuk. Res.* **30,** 240–241
24. Lichter, D. I., Danaee, H., Pickard, M. D., Tayber, O., Sintchak, M., Shi, H., Richardson, P. G., Cavenagh, J., Bladé, J., Façon, T., Niesvizky, R., Alsina, M., Dalton, W., Sonneveld, P., Lonial, S., *et al.* (2012) Sequence analysis of β-subunit genes of the 20S proteasome in patients with relapsed multiple myeloma treated with bortezomib or dexamethasone. *Blood* **120,** 4513–4516
25. Leung-Hagesteijn, C., Erdmann, N., Cheung, G., Keats, J. J., Stewart, A. K., Reece, D. E., Chung, K. C., and Tiedemann, R. E. (2013) Xbp1s-negative tumor B cells and pre-plasmablasts mediate therapeutic proteasome inhibitor resistance in multiple myeloma. *Cancer Cell* **24,** 289–304
26. Orlowski, R. Z. (2013) Why proteasome inhibitors cannot ERADicate multiple myeloma. *Cancer Cell* **24,** 275–277
27. Kuhn, D. J., Berkova, Z., Jones, R. J., Woessner, R., Bjorklund, C. C., Ma, W., Davis, R. E., Lin, P., Wang, H., Madden, T. L., Wei, C., Baladandayuthapani, V., Wang, M., Thomas, S. K., Shah, J. J., Weber, D. M., and Orlowski, R. Z. (2012) Targeting the insulin-like growth factor-1 receptor to overcome bortezomib resistance in preclinical models of multiple myeloma. *Blood* **120,** 3260–3270
28. Bjorklund, C. C., Baladandayuthapani, V., Lin, H. Y., Jones, R. J., Kuiatse, I., Wang, H., Yang, J., Shah, J. J., Thomas, S. K., Wang, M., Weber, D. M., and Orlowski, R. Z. (2014) Evidence of a role for CD44 and cell adhesion in mediating resistance to lenalidomide in multiple myeloma: therapeutic implications. *Leukemia* **28,** 373–383
29. Chorley, B. N., Campbell, M. R., Wang, X., Karaca, M., Sambandan, D., Bangura, F., Xue, P., Pi, J., Kleeberger, S. R., and Bell, D. A. (2012) Identification of novel NRF2-regulated genes by ChIP-Seq: influence on retinoid X receptor α. *Nucleic Acids Res.* **40,** 7416–7429
30. Jaramillo, M. C., and Zhang, D. D. (2013) The emerging role of the Nrf2-Keap1 signaling pathway in cancer. *Genes Dev.* **27,** 2179–2191
31. Chondrogianni, N., and Gonos, E. S. (2007) Overexpression of hUMP1/POMP proteasome accessory protein enhances proteasome-mediated antioxidant defence. *Exp. Gerontol.* **42,** 899–903
32. Wang, X. J., Hayes, J. D., Henderson, C. J., and Wolf, C. R. (2007) Identification of retinoic acid as an inhibitor of transcription factor Nrf2 through activation of retinoic acid receptor α. *Proc. Natl. Acad. Sci. U.S.A.* **104,** 19589–19594
33. De Braekeleer, E., Douet-Guilbert, N., and De Braekeleer, M. (2014) RARA fusion genes in acute promyelocytic leukemia: a review. *Expert Rev. Hematol.* **7,** 347–357
34. Kobayashi, A., Kang, M. I., Okawa, H., Ohtsuji, M., Zenke, Y., Chiba, T., Igarashi, K., and Yamamoto, M. (2004) Oxidative stress sensor Keap1 functions as an adaptor for Cul3-based E3 ligase to regulate proteasomal degradation of Nrf2. *Mol. Cell. Biol.* **24,** 7130–7139
35. Siegel, D. S., Martin, T., Wang, M., Vij, R., Jakubowiak, A. J., Lonial, S., Trudel, S., Kukreti, V., Bahlis, N., Alsina, M., Chanan-Khan, A., Buadi, F., Reu, F. J., Somlo, G., Zonder, J., *et al.* (2012) A phase 2 study of single-agent carfilzomib (PX-171–003-A1) in patients with relapsed and refractory multiple myeloma. *Blood* **120,** 2817–2825
36. Niesvizky, R., Martin, T. G., 3rd, Bensinger, W. I., Alsina, M., Siegel, D. S., Kunkel, L. A., Wong, A. F., Lee, S., Orlowski, R. Z., and Wang, M. (2013) Phase Ib dose-escalation study (PX-171–006) of carfilzomib, lenalidomide, and low-dose dexamethasone in relapsed or progressive multiple myeloma. *Clin. Cancer Res.* **19,** 2248–2256
37. Wang, M., Martin, T., Bensinger, W., Alsina, M., Siegel, D. S., Kavalerchik, E., Huang, M., Orlowski, R. Z., and Niesvizky, R. (2013) Phase 2 dose-expansion study (PX-171–006) of carfilzomib, lenalidomide, and low-dose dexamethasone in relapsed or progressive multiple myeloma. *Blood* **122,** 3122–3128
38. Jakubowiak, A. J., Dytfeld, D., Griffith, K. A., Lebovic, D., Vesole, D. H., Jagannath, S., Al-Zoubi, A., Anderson, T., Nordgren, B., Detweiler-Short, K., Stockerl-Goldstein, K., Ahmed, A., Jobkar, T., Durecki, D. E., McDonnell, K., *et al.* (2012) A phase 1/2 study of carfilzomib in combination with lenalidomide and low-dose dexamethasone as a frontline treatment for

multiple myeloma. *Blood* **120,** 1801–1809
39. Lawasut, P., Chauhan, D., Laubach, J., Hayes, C., Fabre, C., Maglio, M., Mitsiades, C., Hideshima, T., Anderson, K. C., and Richardson, P. G. (2012) New proteasome inhibitors in myeloma. *Curr. Hematol. Malig. Rep.* **7,** 258–266
40. Kumar, S. K., Lee, J. H., Lahuerta, J. J., Morgan, G., Richardson, P. G., Crowley, J., Haessler, J., Feather, J., Hoering, A., Moreau, P., LeLeu, X., Hulin, C., Klein, S. K., Sonneveld, P., Siegel, D., *et al.* (2012) Risk of progression and survival in multiple myeloma relapsing after therapy with IMiDs and bortezomib: a multicenter international myeloma working group study. *Leukemia* **26,** 149–157
41. Jang, J., Wang, Y., Kim, H. S., Lalli, M. A., and Kosik, K. S. (2014) Nrf2, a regulator of the proteasome, controls self-renewal and pluripotency in human embryonic stem cells. *Stem Cells* **32,** 2616–2625
42. Kwak, M. K., Wakabayashi, N., Greenlaw, J. L., Yamamoto, M., and Kensler, T. W. (2003) Antioxidants enhance mammalian proteasome expression through the Keap1-Nrf2 signaling pathway. *Mol. Cell. Biol.* **23,** 8786–8794
43. Pickering, A. M., Linder, R. A., Zhang, H., Forman, H. J., and Davies, K. J. (2012) Nrf2-dependent induction of proteasome and Pa28$\alpha\beta$ regulator are required for adaptation to oxidative stress. *J. Biol. Chem.* **287,** 10021–10031
44. Radhakrishnan, S. K., Lee, C. S., Young, P., Beskow, A., Chan, J. Y., and Deshaies, R. J. (2010) Transcription factor Nrf1 mediates the proteasome recovery pathway after proteasome inhibition in mammalian cells. *Mol. Cell* **38,** 17–28
45. Stessman, H. A., Baughn, L. B., Sarver, A., Xia, T., Deshpande, R., Mansoor, A., Walsh, S. A., Sunderland, J. J., Dolloff, N. G., Linden, M. A., Zhan, F., Janz, S., Myers, C. L., and Van Ness, B. G. (2013) Profiling bortezomib resistance identifies secondary therapies in a mouse myeloma model. *Mol. Cancer Ther.* **12,** 1140–1150
46. Biran, N., Jagannath, S., and Chari, A. (2013) Risk stratification in multiple myeloma, part 1: characterization of high-risk disease. *Clin. Adv. Hematol. Oncol.* **11,** 489–503
47. Moriuchi, M., Ohmachi, K., Kojima, M., Tsuboi, K., Ogawa, Y., Nakamura, N., and Ando, K. (2010) Three cases of bortezomib-resistant multiple myeloma with extramedullary masses. *Tokai J. Exp. Clin. Med.* **35,** 17–20
48. Paton-Hough, J., Chantry, A. D., and Lawson, M. A. (2015) A review of current murine models of multiple myeloma used to assess the efficacy of therapeutic agents on tumour growth and bone disease. *Bone* **77,** 57–68
49. Zhang, N., Liang, J., Tian, Y., Yuan, L., Wu, L., Miao, S., Zong, S., and Wang, L. (2010) A novel testis-specific GTPase serves as a link to proteasome biogenesis: functional characterization of RhoS/RSA-14–44 in spermatogenesis. *Mol. Biol. Cell* **21,** 4312–4324
50. Witt, E., Zantopf, D., Schmidt, M., Kraft, R., Kloetzel, P. M., and Krüger, E. (2000) Characterisation of the newly identified human Ump1 homologue POMP and analysis of LMP7(β5i) incorporation into 20 S proteasomes. *J. Mol. Biol.* **301,** 1–9
51. Fricke, B., Heink, S., Steffen, J., Kloetzel, P. M., and Krüger, E. (2007) The proteasome maturation protein POMP facilitates major steps of 20S proteasome formation at the endoplasmic reticulum. *EMBO Rep.* **8,** 1170–1175
52. Meiners, S., Heyken, D., Weller, A., Ludwig, A., Stangl, K., Kloetzel, P. M., and Krüger, E. (2003) Inhibition of proteasome activity induces concerted expression of proteasome genes and de novo formation of mammalian proteasomes. *J. Biol. Chem.* **278,** 21517–21525
53. Fuchs, D., Berges, C., Opelz, G., Daniel, V., and Naujokat, C. (2008) Increased expression and altered subunit composition of proteasomes induced by continuous proteasome inhibition establish apoptosis resistance and hyperproliferation of Burkitt lymphoma cells. *J. Cell Biochem.* **103,** 270–283
54. Wolf, J., Richardson, P. G., Schuster, M., LeBlanc, A., Walters, I. B., and Battleman, D. S. (2008) Utility of bortezomib retreatment in relapsed or refractory multiple myeloma patients: a multicenter case series. *Clin. Adv. Hematol. Oncol.* **6,** 755–760
55. Hrusovsky, I., Emmerich, B., von Rohr, A., Voegeli, J., Taverna, C., Olie, R. A., Pliskat, H., Frohn, C., and Hess, G. (2010) Bortezomib retreatment in relapsed multiple myeloma–results from a retrospective multicentre survey in Germany and Switzerland. *Oncology* **79,** 247–254
56. Namani, A., Li, Y., Wang, X. J., and Tang, X. (2014) Modulation of NRF2 signaling pathway by nuclear receptors: implications for cancer. *Biochim. Biophys. Acta* **1843,** 1875–1885
57. Magesh, S., Chen, Y., and Hu, L. (2012) Small molecule modulators of Keap1-Nrf2-ARE pathway as potential preventive and therapeutic agents. *Med. Res. Rev.* **32,** 687–726